BRANCH INPUT RESISTANCE AND STEADY ATTENUATION FOR INPUT TO ONE BRANCH OF A DENDRITIC NEURON MODEL

WILFRID RALL *and* JOHN RINZEL

From the Mathematical Research Branch, National Institute of Arthritis, Metabolism, and Digestive Diseases, and the Laboratory of Applied Studies, Division of Computer Research and Technology, National Institutes of Health, Bethesda, Maryland 20014. Dr. Rinzel's present address is the Courant Institute of Mathematical Sciences, New York University, New York 10003.

ABSTRACT Mathematical solutions and numerical illustrations are presented for the steady-state distribution of membrane potential in an extensively branched neuron model, when steady electric current is injected into only one dendritic branch. Explicit expressions are obtained for input resistance at the branch input site and for voltage attenuation from the input site to the soma; expressions for AC steady-state input impedance and attenuation are also presented. The theoretical model assumes passive membrane properties and the equivalent cylinder constraint on branch diameters. Numerical examples illustrate how branch input resistance and steady attenuation depend upon the following: the number of dendritic trees, the orders of dendritic branching, the electrotonic length of the dendritic trees, the location of the dendritic input site, and the input resistance at the soma. The application to cat spinal motoneurons, and to other neuron types, is discussed. The effect of a large dendritic input resistance upon the amount of local membrane depolarization at the synaptic site, and upon the amount of depolarization reaching the soma, is illustrated and discussed; simple proportionality with input resistance does not hold, in general. Also, branch input resistance is shown to exceed the input resistance at the soma by an amount that is always less than the sum of core resistances along the path from the input site to the soma.

INTRODUCTION

It seems now generally accepted that the many synapses distributed over the dendritic surface of a neuron can make significant contributions to the integrative behavior exhibited by this neuron as it responds to various spatiotemporal patterns of afferent input. In some theoretical studies it has been useful to lump the effects of neighboring synapses and to lump regional groupings of the dendritic branches

belonging to a neuron (e.g., Rall, 1962, 1964, 1967). Nevertheless, it is clear that any particular one of these synapses is located upon one particular dendritic branch; also, when a synapse is made with a dendritic spine, that spine is attached to a particular dendritic branch. This gives rise to questions about the input resistance that would be "seen" or confronted by a particular synapse on a particular dendritic branch. Questions arise also about the amplitude of membrane depolarization generated at the synaptic site, and about the attenuation of amplitude as this membrane depolarization spreads (electrotonically) from the synaptic site to other locations, both in the same dendritic tree, at the neuron soma, and in other dendritic trees of the same neuron. Such questions have been noted and discussed, for example, by Katz and Miledi (1963, p. 419), Arshavskii et al. (1965), Rall (1967; 1970, p. 184), and Kuno (1971).

This is the first of several closely related papers which provide mathematical solutions and contribute biophysical intuition toward the understanding of effects of synaptic input to one branch of an extensively branched neuron model. This first paper is restricted to the steady-state problem. For a steady current applied across the membrane at one site in one branch of the neuron model, the complete steady-state solution for the distribution of electrotonic potential throughout all branches and trees of the neuron model is obtained. This steady-state solution provides expressions for branch input resistance and for steady-state attenuation of electrotonic potential from the branch input site to the neuron soma; numerical examples are tabulated, illustrated, and discussed.

The second paper[1] treats the corresponding transient problem, for the injection of a brief current at the branch input site. Our solution of this more difficult problem depends upon the conceptual approach (mathematical superposition of simpler boundary value problems) that is introduced, illustrated, and discussed in the first paper. In addition to providing a mathematical derivation of the required transient response functions, the second paper also illustrates and discusses specific computed examples.

Subsequent papers of this series will deal with the additional theoretical complications involved in treating synaptic input to a dendritic spine. The effect of a synaptic excitatory conductance at the spine head is coupled to the dendritic branch by means of the spine stem current. Our solution of this problem depends partly upon the transient response functions derived in the second paper of this series. Also, the steady-state interpretations of synaptic input to a dendritic spine make use of the steady-state results in the first paper of this series. A consideration of these theoretical results in relation to recent neuroanatomical studies of dendritic spines has led to a recognition of possible functional implications of spine stem resistance; a paper presenting and discussing these implications is in preparation.

---

[1] Rall, W., and J. Rinzel. Manuscript in preparation.

Brief communications of various portions of this research have already been presented on several occasions.[2]

ASSUMPTIONS OF NEURON MODEL

Symmetry and Idealized Branching

Much of our biophysical intuition and many of our mathematical results have been facilitated by several assumptions of symmetry in our idealized neuron models. If we had been interested only in the steady-state problem, we could have dispensed with these symmetry assumptions completely: we could have solved the problem by the same stepwise procedure (which permits arbitrary branch lengths and diameters) that was outlined earlier (Rall, 1959) for the case of steady current injection at a neuron soma. The symmetry assumptions are of greatest value in obtaining the transient solutions;[1] they permit us to apply the mathematical principle of superposition to construct the solution of a complicated boundary value problem as a combination of several simpler boundary value problems. Because it simplifies our exposition of the particular superpositions we have used, we have chosen to introduce the method in this steady-state paper. Also, we simplify our presentation by beginning with more severe symmetry assumptions than superposition actually requires; the effects of relaxing the severity of these assumptions are examined later in the Appendix.

Most of our results are expressed for an idealized neuron model composed of several equivalent dendritic trees (N in number) in which there are several orders (M) of symmetric dendritic branching. A diagram of one particular example (Fig. 1 A) shows six equal dendritic trees in which there are two orders of symmetric dendritic branching. It should be pointed out immediately that the angles between the trees and between the branches are of no importance. These angles do not enter into any of the mathematics.[3] It is the lengths and diameters of the trunks and branches that are important. Fig. 1 A is intended merely to bring out the equivalences between corresponding lengths and diameters. The soma of this neuron model is represented by the common origin of the six dendritic trees.

In addition to the symmetry assumptions already noted, we have restricted our treatment to dendritic trees whose branch diameters satisfy the constraint for trans-

---

[1] The use of symmetry and superposition to obtain these solutions was included in a presentation for the American Association for the Advancement of Science Symposium on Some Mathematical Questions in Biology, Boston, December, 1969. The mathematical and numerical treatment of coupling the dendritic spine to a branch of the model was presented at the Society for Industrial and Applied Mathematics National Meeting, Denver, June, 1970. Functional implications for dendritic spines were presented at the 25th International Congress of Physiological Sciences, Munich, July, 1971, and at the first annual meeting of the Society for Neuroscience, Washington, D. C., October, 1971.

[3] This follows from the assumption of extracellular isopotentiality; see Other Simplifying Assumptions section below.

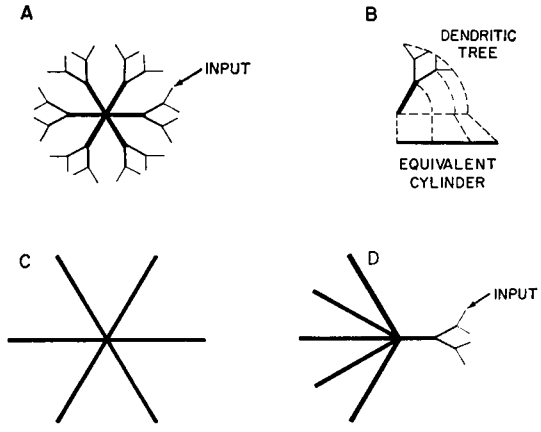

FIGURE 1 Diagrams illustrating features of the idealized neuron model. A represents the neuron model composed of six identical dendritic trees. B indicates the relation of a dendritic tree to its equivalent cylinder. C represents the same model as A, with each dendritic tree replaced by an equivalent cylinder. D represents the same model as A and C, with dendritic branching shown explicitly only for the tree which receives input current injected into the terminal of one branch; the five other trees of the model are represented by their equivalent cylinders, here shown gathered together. In diagrams A, C, and D, the point of common origin of the trees or equivalent cylinders is regarded as the neuron soma; see text.

formations between a tree and an equivalent cylinder (Fig. 1 B; also Rall, 1962, 1964). Except in the Appendix, we have assumed symmetric bifurcations that yield daughter branches of equal diameter. Together, these assumptions imply that at every branch point, each daughter branch diameter is about 63% of its parent branch diameter; strictly, the requirement is that the 3/2 power of each daughter diameter be exactly half as great as the 3/2 power of its parent diameter. With such branching, an entire dendritic tree can be shown to be mathematically equivalent to a cylinder (Rall, 1962); increments Δx of actual dendritic length are expressed as increments of electrotonic length, $\Delta X = \Delta x/\lambda$, where λ is the characteristic length of each cylinder as defined below. This equivalence applies to spatio-temporal spread from the trunk into the dendritic branches; it applies also to spread from the dendrites to the trunk, when the input is delivered equally to all terminal branches of that dendritic tree.

The equivalent cylinder concept can be used to reduce the idealized (branched) neuron model of Fig. 1 A to simpler versions (Figs. 1 C and D) for appropriate conditions. Thus, for example, if current is injected equally to all terminal branches of just one of the six dendritic trees of Fig. 1 A, this tree can be treated as an equivalent cylinder which receives input at its distal end. The origin of this cylinder can be coupled to the origins of five other equivalent cylinders, as in Fig. 1 C. These other cylinders have the same dimensions as the input cylinder but differ in receiving no input at their distal ends; they receive equal shares of the current that reaches

them at their common origin (soma) from the input cylinder. The six cylinders in Fig. 1 C represent the same neuron model as that in Fig. 1 A; the existence of the branches makes no difference under the stated condition of input delivered equally to all terminal branches of the one tree. However, when the input current is injected to only one branch terminal of one dendritic tree, it is necessary to include the branching details of that tree but not the branching of the other trees, as shown in Fig. 1 D. The five equivalent cylinders which do not receive input have been oriented more together in this figure to emphasize their equivalence with each other in sharing equally the current that flows to the origin (soma) from the input tree; the angles between the cylinders have no other significance, as noted earlier.[8] This last case (Fig. 1 D) is an illustrative example of the problem we solve below.

Other Simplifying Assumptions

Here we briefly note several other simplifying assumptions of dendritic neuron models (cf., Rall, 1959, 1962). All dendritic trunks and branches are treated as cylinders of uniform passive nerve membrane. Extracellular resistivity is neglected, implying extracellular isopotentiality. This, together with the usual core conductor assumptions, permits each cylinder to be treated as a one-dimensional cable of finite length (see Rall [1969 *b*] for discussion and references). At all branch points, membrane potential is assumed to be continuous, and core current is conserved. Dendritic terminals are assumed to be "sealed" or "insulated," implying zero leakage current across the terminal membrane; except for a terminal where current is injected, this implies a zero slope ($dV/dX = 0$) boundary condition, just inside (not across) the terminal membrane.

The assumption of extracellular isopotentiality brings with it several useful simplifications. It means that spatial orientation of the dendritic trees and branches can have no effect upon the distribution of membrane potential over the dendritic surfaces; only electrotonic distances and boundary conditions are important. It also provides simpler expressions for the characteristic length λ and for the various input resistances. It should be noted that this assumption represents a good approximation for some experimental situations, but not for others. For a single dendritic neuron placed in a volume conductor (which is assumed not to be subjected to an externally applied electric field) the current flow generated by activity of that neuron results in gradients of extracellular potential that are negligible relative to the much larger gradients of intracellular potential along the intracellular core resistance and across the relatively large membrane resistance (for estimates, see Rall, 1959, 1969 *b*). When extracellular space is severely restricted, however, either by glial sheaths or by simultaneous activity in a large population of closely packed cells, extracellular potential gradients can become comparable with or even greater than the intracellular potential gradients; see, for example, synchronous activity of granule cells in olfactory bulb (Rall and Shepherd, 1968, pp. 887–890, 901–904).

Under such conditions, one must avoid assuming extracellular isopotentiality and assume an appropriate extracellular resistance per unit length for each cylinder; also, the effects of tree and branch orientation would then need to be considered.

Because it might be objected that we should not treat the soma as merely the point of common origin of the dendritic trees, we comment. The superposition methods of this paper and its transient sequel would lose much of their simplicity if a lumped soma were explicitly included at the origin of the neuron model. This can be verified by examining the effect of a lumped soma upon previously published theoretical transient results (Rall, 1969 *a*, pp. 1492–1496; see also Rall, 1960, as well as Jack and Redman, 1971). Our present assumption of a point soma can be qualified with the thought that a finite soma surface area could be designated, if needed, as being composed of several initial length increments, one from each dendritic trunk. Finally, we note also that the neuron model of the present paper does not include an axon- or a spike-generating locus; our focus of attention is upon the contribution of passive membrane electrotonus to the integrative properties of the extensively branched neuron model.

SYMBOLS

For Membrane Cylinders

$V_m = V_i - V_e$	Membrane potential, as intracellular minus extracellular electric potential; (volts).
$V = V_m - E_r$	Electrotonic potential, as deviation of membrane potential from its resting value E_r; (volts).
R_i	Resistivity of intracellular medium; (ohms centimeters).
R_m	Resistance across a unit area of membrane; (ohms square centimeters).
d	Diameter of membrane cylinder; (centimeters).
$r_i = 4R_i/(\pi d^2)$	Core resistance per unit length; (ohms centimeters^{-1}).
$\lambda = [(R_m/R_i)(d/4)]^{1/2}$	Characteristic length of membrane cylinder, when extracellular resistance is neglected; (centimeters).
x	Actual distance along a cylinder axis; (centimeters).
$\Delta X = \Delta x/\lambda$	Increment of electrotonic distance; (dimensionless).
$X = \int_0^x (1/\lambda)\, dy$	Electrotonic distance from origin; in a tree, λ changes at each branch point; (dimensionless).
$R_\infty = \lambda r_i = (2/\pi)(R_m R_i)^{1/2}(d)^{-3/2}$	Input resistance at origin of membrane cylinder of semi-infinite length; (ohms).

For Membrane Cylinders of Finite Length

L	Electrotonic distance from origin ($X = 0$) to the end of cylinder ($X = L$).
$R_{CL,\,ins}$	Input resistance at end ($X = L$) for a *cylinder insulated* ($dV/dX = 0$) at the origin; Eq. 7.
$R_{CL,\,clp}$	Input resistance at end ($X = L$) for a *cylinder clamped* ($V = 0$) at the origin; Eq. 9.

For Idealized Neuron Model

N	Number of equivalent dendritic trees (or their equivalent cylinders) that are coupled at $X = 0$.
L	Electrotonic length of each of those trees or equivalent cylinders.
M	Number of orders of symmetric branching, specifically in the dendritic tree which receives the input.
X_1	Electrotonic distance from the origin to the first point of branching.
X_k	Electrotonic distance from the origin to the kth-order branch points.
$R_{T\infty}$	Value of R_∞ for the *trunk* cylinder of one dendritic tree.
R_N	Whole *neuron* input resistance at the point ($X = 0$) of common origin of the N trees or equivalent cylinders; Eq. 11.
R_{NCL}	Input resistance at the end ($X = L$) of one equivalent *cylinder* of the neuron model, for current applied as in Fig. 2 F; Eq. 14.
R_{BL}	Input resistance at the end ($X = L$) of one terminal *branch* of the neuron model, for current applied as in Figs. 1 A and D; Eq. 22.
V_{BL}	Steady value of V at input *branch* terminal.
V_O	Steady value of V at the *origin* of the neuron model.
$AF_{BL/O} = V_{BL}/V_O$	Attenuation factor from input branch terminal to soma; Eq. 26.

For the Discussion

V_{in}	Steady value of V at some synaptic site.
R_{in}	Input resistance at this synaptic site.
g_e	Synaptic excitatory conductance at this synaptic site.
$V_e = E_e - E_r$	Synaptic excitatory equilibrium potential, being the difference between the excitatory emf and the resting emf.
$(V_e - V_{\text{in}})$	Effective steady driving potential for synaptic current.
V_{in}/V_e	Normalized steady synaptic depolarization; Eq. 32.
$\Delta X = L/(M + 1)$	For equal electrotonic increments.

THEORY

For the usual assumptions of one-dimensional cable theory, steady-state distributions of membrane potential along the length of a passive membrane cylinder must satisfy the ordinary differential equation

$$d^2V/dX^2 - V = 0, \tag{1}$$

where X and V are explicitly defined in the list of Symbols. Because we wish to exploit even and odd symmetry about the origin, we express the general solution of Eq. 1 in terms of hyperbolic functions,[4] as follows,

$$V = A \sinh X + B \cosh X, \tag{2}$$

[4] The hyperbolic sine and cosine are defined and tabulated in standard mathematical tables. Because $\sinh(-X) = -\sinh(X)$, this function has odd symmetry about the origin. Because $\cosh(-X) = \cosh(X)$, this function has even symmetry about the origin.

where A and B are arbitrary constants to be determined by the boundary conditions.

When a steady current I is injected at the terminal ($X = L$) of a cylinder of finite length, the terminal boundary condition can be expressed

$$dV/dX = IR_\infty , \qquad \text{at } X = L, \tag{3}$$

where R_∞ represents the input resistance for a semi-infinite length of such a cylinder. It may be noted that both the diameter and the materials of the cylinder are included in the definition of R_∞ ; see the list of Symbols. To understand this boundary condition, it is helpful to note that the intracellular (core) current (flowing parallel to the cylinder axis and taken as positive when in the direction of increasing x) can be given several alternative[5] expressions

$$(-dV_i/dx)/r_i = (-dV_i/dX)/(\lambda r_i) = (-dV/dX)/R_\infty .$$

When the injected current is positive, the resulting core current is negative, because it must flow from $X = L$ toward the origin. Furthermore, we assume that none of the injected current can leak out through the sealed terminal of the cylinder; therefore, the core current must equal exactly $-I$ at $X = L$, and Eq. 3 must hold. It should be added that for a cylinder which extends from the origin to a terminal at $X = -L$, the sign becomes reversed, because a positive current injected at this terminal would result in a positive core current flowing from $X = -L$ toward the origin. Thus, the boundary condition for current injection at $X = -L$ differs from Eq. 3 by a minus sign.

Even Symmetry for 2L; or Length L Insulated at the Origin

For a cylinder of length $2L$ diagram A in Fig. 2 illustrates the case of even symmetry, where the same steady current $I/2$ is injected at both ends ($X = \pm L$) of the cylinder. This symmetry requires[4] that $A = 0$ in Eq. 2; the value of B can be determined from the boundary condition at either end. Because the core current at $X = L$ must equal minus $I/2$ in this example, we see (from Eq. 3, above) that the boundary condition here can be expressed

$$dV/dX = (I/2)R_\infty , \qquad \text{at } X = L. \tag{4}$$

Together with $A = 0$ in Eq. 2, this boundary condition implies that $B = (I/2)R_\infty/$

[5] The first expression simply represents Ohm's Law. The second uses the substitution, $dx = \lambda dX$, which follows from the definition of X. The third expression depends upon two substitutions: $\lambda r_i = R_\infty$, by definition, and $dV_i/dX = dV/dX$, because $V = V_i - V_e - E_r$, and both V_e and E_r are assumed to be constants (independent of X).

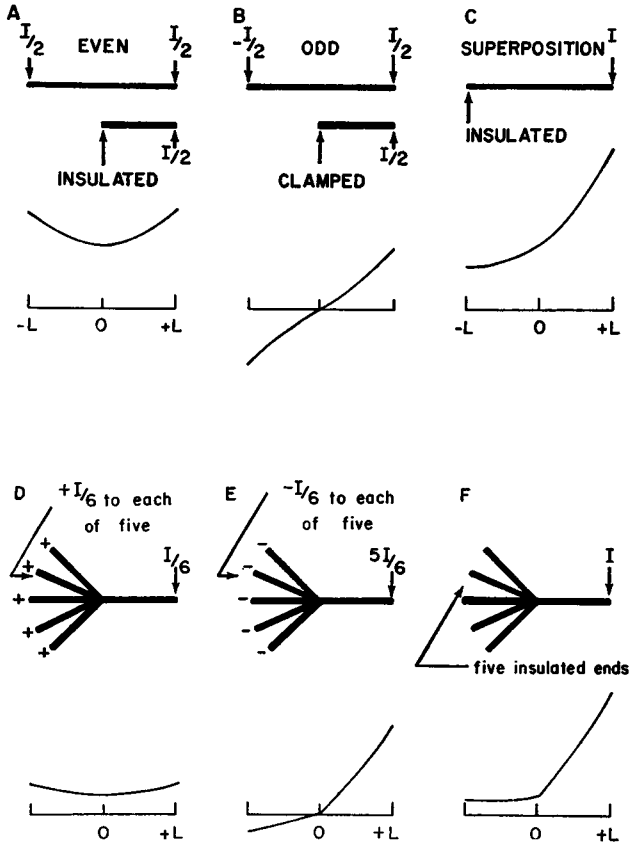

FIGURE 2 Diagrams illustrating superposition of component boundary value problems characterized by even and odd symmetry; see text. A, B, and C refer to a cylinder of length $2L$. A shows even symmetry for equal source currents at both ends; the graph of V with distance shows zero slope at origin ($X = 0$), corresponding also to insulated boundary condition at origin. B shows odd symmetry for a source current at $X = L$ with a matching sink current at $X = -L$; the graph shows $V = 0$ at origin, corresponding also to voltage-clamped boundary condition at origin. C shows the superposition of A and B; the graph shows zero slope at $X = -L$, corresponding to insulated boundary condition at $X = -L$. D, E, and F refer to a neuron model composed of six equal cylinders of length L like Fig. 1 C; one cylinder extends to the right, to distinguish it from the other five, shown gathered to the left of the common origin. D shows even symmetry for equal source currents $I/6$ applied to the distal ends of all six cylinders; the graph shows zero slope at the origin. E shows the result of five source-sink current pairs, where one cylinder receives all five source currents, while each of the other five cylinders receives one of the $(-I/6)$ sink currents; the graph shows discontinuous slope at origin, where the one cylinder has a slope which is five times as steep as that in each of the five other cylinders. F shows the superposition of D and E, where the resultant current is all applied to one cylinder; the graph shows that the five other cylinders satisfy a zero slope (insulated) boundary condition at their distal ends; graph also shows a fivefold discontinuity of slope at the origin, in agreement with E.

sinh L, and that the solution for this case of even symmetry can be expressed

$$V(X) = (I/2)R_\infty \cosh X/\sinh L, \tag{5}$$

for the entire range, $-L \leq X \leq L$. It should be noted that the case of even symmetry necessarily implies the condition

$$dV/dX = 0, \qquad \text{at } X = 0, \tag{6}$$

which corresponds also to an insulated or sealed boundary at $X = 0$, as noted in Fig. 2 A.

The input resistance at $X = L$, for this case of a cylinder insulated at the origin, is the ratio of the steady input voltage, $V(X)$ at $X = L$, to the steady input current $I/2$. It follows from Eq. 5 that this input resistance can be expressed

$$R_{CL,\ \mathrm{ins}} = R_\infty \coth L. \tag{7}$$

For example, if $L = 1.0$, this input resistance is 1.313 times R_∞. For values of L greater than 2.65, this resistance differs from R_∞ by less than 1%.

Odd Symmetry for 2L; or Length L Clamped at the Origin

For a cylinder of length $2L$ diagram B in Fig. 2 illustrates the case of odd symmetry, where a steady source current $I/2$ is injected at $X = L$, and a matching steady sink current $-I/2$ is applied at $X = -L$. This odd symmetry requires that $B = 0$ in Eq. 2; the value of A can be determined from the boundary condition at either end. The boundary condition at $X = L$ can be expressed in the same form as Eq. 4, but here, with $B = 0$ in Eq. 2, this boundary condition implies that $A = (I/2)R_\infty/\cosh L$, and that the solution for this case of odd symmetry can be expressed

$$V(X) = (I/2)R_\infty \sinh X/\cosh L, \tag{8}$$

for the entire range, $-L \leq X \leq L$. It should be noted that the case of odd symmetry necessarily satisfies the condition $V = 0$ at $X = 0$ which is equivalent to a voltage-clamped boundary condition at $X = 0$, as noted in Fig. 2 B.

Setting $X = L$ in Eq. 8, we see that the input resistance at $X = L$ can be expressed, for this case of a cylinder clamped ($V = 0$) at the origin, as

$$R_{CL,\ \mathrm{clp}} = R_\infty \tanh L. \tag{9}$$

For example, if $L = 1.0$, this input resistance is 0.762 times R_∞. For values of L greater than 2.65, this resistance differs from R_∞ by less than 1%.

Whole Neuron Input Resistance at Origin (Soma) of Neuron Model

Consider a neuron model composed of N equal dendritic trees coupled to a common origin (Fig. 1 A). Each tree has a trunk whose diameter and materials can be characterized by $R_{T\infty}$, the input resistance at the origin of a trunk cylinder extended to semi-infinite length. Each dendritic tree is assumed to have a finite electrotonic length L and, in those situations (such as current injection at the origin) where it is not necessary to distinguish between separate dendritic branches, each dendritic tree can be represented as an equivalent cylinder (Figs. 1 B and C) of electrotonic length L. We assume all dendritic terminals to have sealed (insulated) ends; this implies a zero slope ($dV/dX = 0$) boundary condition at $X = L$. If the current, I is injected at the common origin of N such cylinders, I/N flows into each cylinder, and the steady potential distribution can be expressed, for each cylinder, as

$$V(X) = (I/N)R_{T\infty} \cosh (L - X)/\sinh L, \tag{10}$$

which satisfies the boundary conditions at $X = 0$ and at $X = L$. The whole neuron input resistance R_N at the origin of this model is the ratio of the steady input voltage $V(X)$ at $X = 0$ to the steady input current I. It follows from Eq. 10 that this input resistance can be expressed

$$R_N = (R_{T\infty} \coth L)/N. \tag{11}$$

For example, consider $L = 1.0$ and $N = 6$; then R_N is 0.219 times $R_{T\infty}$. For values of L greater than 2.65, R_N differs from $R_{T\infty}/N$ by less than 1%.

Effect of Restricting Input Current to One Cylinder of Neuron Model

Suppose that a steady current I/N is injected at the end of each cylinder, as illustrated in Fig. 2 D for the case of $N = 6$. Then there is even symmetry with respect to the origin, and Eqs. 4–7 apply, with I/N replacing $I/2$, and $R_{T\infty}$ replacing R_∞. Next, instead of this even symmetry, suppose that a steady source current I/N is injected at the end of only one cylinder, while a steady sink current $-I/N$ is applied to the end of one other cylinder. For the special case of $N = 2$, this is exactly the same as Fig. 2 B and Eqs. 8 and 9. For N greater than 2, it should be noted that the additional cylinders would not be disturbed by the single source-sink pair just described.[6] Thus, as shown in Fig. 2 E, we can superimpose $(N - 2)$ additional source-sink pairs, with the result that one cylinder receives a combined source current $(N - 1)I/N$ at its end $X = L$ while each of the $(N - 1)$ other cylinders receive separate sink currents each of which equals $-I/N$; note that this

[6] The several cylinders are connected only at the origin, and the source-sink pair satisfies two conditions: $V = 0$ at the origin, and the current reaching the origin from the source is exactly matched by the current flowing from the origin toward the sink.

superposition of source-sink pairs preserves the voltage-clamped condition ($V = 0$) at the origin (Fig. 2 E).

Now we can superimpose the N sources of Fig. 2 D with the $(N - 1)$ source-sink pairs of Fig. 2 E to obtain the combined result of Fig. 2 F, where one cylinder receives a combined current injection I at $X = L$, while the complete cancellation of the source and sink currents at the ends of the $(N - 1)$ other cylinders implies that their ends receive zero resultant input current and thus correspond to insulated ends.

As is indicated in Fig. 2 F, it is convenient to let the input cylinder be represented by positive values of X, and to let the $(N - 1)$ other cylinders be represented by negative values of X. Thus, the superimposed solution can be represented mathematically (using Eqs. 5 and 8 with $I/2$ replaced by I/N, and R_∞ replaced by $R_{T\infty}$) by the following two expressions: for the input cylinder (i.e., for $0 \leq X \leq L$),

$$V(X) = (I/N)R_{T\infty} [\cosh X/\sinh L + (N - 1) \sinh X/\cosh L], \qquad (12)$$

while, for each of the $(N - 1)$ other cylinders (i.e., for $-L \leq X \leq 0$),

$$V(X) = (I/N)R_{T\infty} [\cosh X/\sinh L + \sinh X/\cosh L]. \qquad (13)$$

It may be noted that this steady-state solution does satisfy continuity of V and conservation of core current at the origin; it also satisfies the current input boundary condition ($dV/dX = IR_{T\infty}$) at $X = L$ of the input branch, as well as the zero slope boundary condition at each terminal ($X = -L$) of the $N - 1$ other cylinders of the neuron model.

Setting $X = L$ in Eq. 12 and dividing by the steady input current I we see that the input resistance at $X = L$ of the input cylinder can be expressed, for this case of current injection at the end of one cylinder of the neuron model, as

$$R_{NCL} = R_{T\infty}[\coth L + (N - 1) \tanh L]/N. \qquad (14)$$

It can be seen that for $N = 1$, this equation reduces to Eq. 11, as it should. Also, for large L, where both the hyperbolic tangent and hyperbolic cotangent differ negligibly from unity, this resistance differs negligibly from $R_{T\infty}$, as would be expected from the physical intuitive consideration that the boundary condition at the origin should have negligible effect upon the terminal input resistance when L is large enough. Additional insight into this result can be obtained by referring this result to the insulated and "clamped" (even and odd) results of Eqs. 7 and 9; then the present result can be expressed

$$R_{NCL} = [1/N]R_{CL,\,\mathrm{ins}} + [(N - 1)/N]R_{CL,\,\mathrm{clp}}, \qquad (15)$$

where we have identified $R_{T\infty}$ (of Eq. 14) with R_∞ (of Eqs. 7 and 9).

A physical interpretation of this result is that a fraction $1/N$ of the input current is completely dissipated in the input cylinder (as though there were insulation at the origin; see Figs. 2 A and D), while the remaining fraction $(N - 1)/N$ of the input current dissipates partly in the input cylinder and partly in the other cylinders (as though the origin were clamped to $V = 0$; see Fig. 2 E).

In view of earlier Eq. 11 for the whole neuron input resistance R_N at the origin, we can use Eq. 14 to express the ratio

$$R_{NCL}/R_N = 1 + (N - 1)(\tanh L)^2. \tag{16}$$

For example, if $L = 1.0$ and $N = 6$, the input resistance R_{NCL} defined by Eqs. 14–16 is 3.9 times R_N, or 0.86 times $R_{T\infty}$. For large values of L, the input resistance ratio of Eq. 16 is nearly N.

It is also interesting to note that the special case $N = 2$ which reduces Fig. 2 F to Fig. 2 C, also reduces Eq. 14 to the simpler expression

$$\begin{aligned} R_{2CL} &= R_{T\infty}(\coth L + \tanh L)/2 \\ &= R_{T\infty} \coth (2L), \end{aligned} \tag{17}$$

where the second form follows from a standard identity. This agrees, as it should, with Eq. 7 for a doubling (from L to $2L$) of the distance from the insulated end to the input end of a cylinder; compare Fig. 2 C with the right half of Fig. 2 A.

Effect of Restricting Input Current to One Dendritic Branch Terminal

We consider first the case where there is only one order of symmetric dendritic branching. Diagrams A, B, and C in Fig. 3 illustrate the superposition method for this case. If both branch terminals of one tree receive the same steady input current $I/2$ (as in Fig. 3 A) the distribution of steady membrane potential must be exactly the same in both branches. Given that the branch diameter satisfies the constraint for transformation of this tree to an equivalent cylinder, this case is equivalent to the injection of I at $X = L$ in the equivalent cylinder. In other words, the case of Fig. 3 A is equivalent to that of Fig. 2 F, and the steady-state solution is the same as that given by eqs. 12 and 13.

Now we consider the particular kind of odd symmetry illustrated by Fig. 3 B, where a steady source current $I/2$ is injected at one branch terminal, while a matching steady sink current $-I/2$ is applied at the other branch terminal. Let $X = X_1$, define the (first-order) branch point. The odd symmetry between the two branches implies that $V = 0$ at $X = X_1$, and that all of the current flowing to $X = X_1$ from the source branch must exactly equal all of the current flowing from $X = X_1$ into the sink branch. This source-sink pair supplies no current or voltage to the trunk or the other trees, which is why they are dotted in Fig. 3 B. The distribution of steady

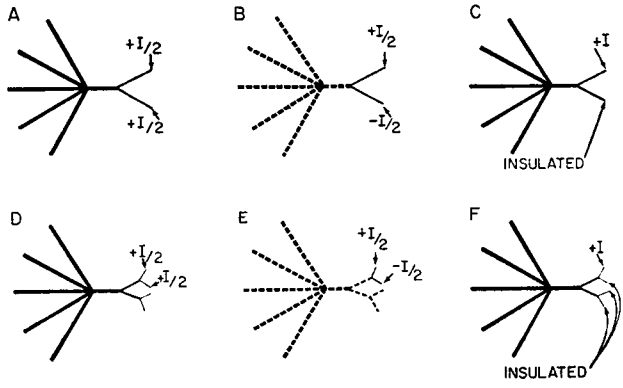

FIGURE 3 Extension of superposition method to dendritic branching in one tree; see text. Diagrams A, B, and C, represent the simplest case of only one order of branching, with a pair of equal branches. A shows even branch symmetry, with equal source currents to both branch terminals. B shows odd branch symmetry, with a source current applied to one branch terminal and a matching sink current applied to the other; no current flows in the dotted regions. C shows the superposition of A and B, where the resultant current is all applied to one first-order branch terminal. Diagrams D, E, and F represent the extension to second-order branching. D shows even branch symmetry only for the pair of secondary branches belonging to one primary branch, with equal sources currents to both of these secondary branch terminals. E shows odd branch symmetry, for a source-sink current pair applied to one pair of secondary branch terminals. F shows the superposition of D and E, where the resultant current is all applied to a single secondary branch terminal.

potential in the source branch, due to this source-sink pair alone, can be expressed

$$V(X) = (I/2)(2R_{T\infty}) \sinh (X - X_1)/\cosh (L - X_1), \qquad (18)$$

for the range, $X_1 \leq X \leq L$; the sister (sink) branch has corresponding negative values. This odd symmetry may be compared with that of Fig. 2 B and Eq. 8. Here, we note that $(I/2)$ is the amount of the source current, and that $(2R_{T\infty})$ is the R_∞ value for each branch cylinder; this R_∞ value follows from the equivalent cylinder constraint which requires that symmetric branches each have a $d^{3/2}$ value equal to half the trunk value.

Steady-State Solution for One Order of Branching

By superimposing the odd branch symmetry of Fig. 3 B with the even branch symmetry of Fig. 3 A, we obtain the case of input to a single branch of first order, Fig. 3 C. Within this input branch, the resultant solution is given by the sum of Eqs. 12 and 18 (i.e., the righthand sides) for the range $X_1 \leq X \leq L$. For the sister branch, the solution is given by Eq. 12 minus Eq. 18. For the trunk $(0 \leq X \leq X_1)$, Eq. 12 alone is still the solution; also, for the $(N - 1)$ other trees, Eq. 13 is still the solution assuming $(-L \leq X \leq 0)$ as before.

This result has the interesting implication that the solution in the trunk and in the other trees is completely unaffected by whether the input current I is injected

entirely into one branch terminal or divided equally between the two branch terminals, and this is easily generalized to include any apportionment of this input current between these two branch terminals.

Extension to Higher Orders of Branching

Diagrams D, E, and F of Fig. 3 illustrate the additional superposition required when we add a second order of symmetric branching. When the same steady input current $I/2$ is delivered to the terminals of the two secondary branches belonging to the same parent primary branch (Fig. 3 D), the distribution of steady membrane potential is the same in both of these secondary branches and is equivalent to that of Fig. 3 C, just solved above.

Now we consider the case of odd symmetry between this pair of secondary branches (Fig. 3 E), with a steady source current $I/2$ injected at the terminal of one secondary branch, while a matching steady sink current $-I/2$ is applied at the terminal of its sister branch. Let $X = X_2$ be the electrotonic distance, from origin to second-order branch point. In analogy with the previously considered odd symmetry between a pair of primary branches (Fig. 3 B), this case of odd symmetry between a pair of secondary branches has $V = 0$ at $X = X_2$, and supplies no current or voltage to any of the regions shown dotted in Fig. 3 E. The distribution of steady potential in the source branch, due to this source-sink pair alone, will be expressed in the more general form that applies to a branch pair of kth order, where the particular case $k = 2$ corresponds to the secondary branches of Fig. 3 E; this general form is

$$V(X) = (I/2)(2^k R_{T\infty}) \sinh (X - X_k)/\cosh (L - X_k), \qquad (19)$$

for the range, $X_k \leq X \leq L$; the sister (sink) branch has corresponding negative values. We note that $(I/2)$ is the amount of the source current (of the source-sink pair), and that $(2^k R_{T\infty})$ is the R_∞ value for a kth-order branch, on the assumption of symmetric branching in a tree satisfying the equivalent cylinder constraint. It may be noted that Eq. 19 agrees, when $k = 1$, with Eq. 18, as it should.

The case of input restricted to the terminal of a single secondary branch (Fig. 3 F) is obtained by superimposing the odd (secondary branch) symmetry of Fig. 3 E with the even (secondary branch) symmetry of Fig. 3 D, where we have already noted that the latter is equivalent to the case of Fig. 3 C, for one order of branching. This method can now be generalized by using Eq. 19 in successive superpositions, as the order k is stepped from 1 to M in unit steps.

Steady-State Solution for Branch Terminal Input with M Orders of Branching

When there are M orders of symmetric branching in the input tree, the method of successive superpositions (using Eqs. 12 and 19) leads to the following general

expression for the distribution of potential in this neuron model when the steady current I is injected only at the terminal of one branch,

$$V(X) = IR_{T\infty}\left\{\frac{\cosh X}{N \sinh L} + \frac{A \sinh X}{N \cosh L} + \sum_{k=1}^{M} 2^{(k-1)} \frac{B_k \sinh (X - X_k)}{\cosh (L - X_k)}\right\}, \quad (20)$$

where A and B_k are simple constants whose values are specified according to location, as follows:

in the input tree	$A = N - 1$;
in the input branch	$B_k = 1$, for all k from 1 to M;
in the sister branch	same, except $B_M = -1$;
in the parent branch	same, except $B_M = 0$;
in first cousin branches	same, except $B_M = 0$, and $B_{M-1} = -1$;
in grandparent branch	same, except $B_M = 0$, and $B_{M-1} = 0$;
. . .	
in the input trunk	$B_k = 0$, for all k; (cf. Eq. 12);
in the other trees	$A = 1$, assuming,[7] $X < 0$, and $B_k = 0$, for all k; (cf. Eq. 13).

A specific example of such solutions is presented and illustrated in the Results section below.

By differentiating Eq. 20 with respect to X and setting $X = L$, we can verify that the boundary condition at the input-receiving branch terminal is correctly satisfied; thus

$$(dV/dX)_{X=L} = IR_{T\infty}\left\{(1/N) + (N - 1)/N + \sum_{k=1}^{M} 2^{(k-1)}\right\}$$

$$= 2^M IR_{T\infty}, \quad (21)$$

which is I times the R_∞ value of a Mth-order branch cylinder, as it should be, according to Eq. 3. For the sister branch, the corresponding expression for its terminal boundary condition reduces to zero because the last term of the summation has a minus sign. A zero slope boundary condition is similarly satisfied at the ends of all terminal branches (except the input branch) of this neuron model. The other boundary conditions, continuity of V and conservation of core current at every branch point, have been satisfied also by the method of superposition used; each odd function that was superimposed at a branch point contributed zero to the value of V at that point, and contributed a source-sink pair of currents whose net contribution was also zero at that point.

Input Resistance for Current Injected to a Single Branch Terminal

We can now give the general expression for the input resistance R_{BL} for current injected at the terminal ($X = L$) of one dendritic branch of a neuron model com-

[7] This sign convention agrees with Figs. 2 D, E, F and with Eq. 13. Alternatively, if the other trees are represented by positive values of X, as in Fig. 4 and in expression 27 below, then $A = -1$.

posed of N equal dendritic trees, with M orders of symmetric dendritic branching (which satisfy the equivalent cylinder constraint). By setting $X = L$ in Eq. 20 (for the input branch) and dividing by the steady input current I we obtain the input resistance

$$R_{BL} = R_{T\infty}\left\{\frac{\coth L}{N} + \frac{(N-1)\tanh L}{N} + \sum_{k=1}^{M} 2^{(k-1)} \tanh (L - X_k)\right\}. \quad (22)$$

For the special case of no dendritic branching, $M = 0$ and the summation expression in Eq. 22 contributes nothing; this equation then reduces to Eq. 14. Also, the special case of a long input branch makes all of the hyperbolic tangent and hyperbolic cotangent values close to unity; then (as seen with Eq. 21) the expression for R_{BL} reduces essentially to $2^M R_{T\infty}$, which is the R_∞ value of an Mth-order branch cylinder, as would be expected from physical intuitive considerations.

In this expression, the size and the materials of the neuron model are incorporated in $R_{T\infty}$, which is the limiting value of the input resistance of a dendritic trunk cylinder, when extended to semi-infinite length. In experimental situations, however, it is the value of the whole neuron input resistance R_N at the soma that is the most useful reference value. Also, referring to Eq. 11 for R_N, we see that it is not difficult to express the ratio of these two input resistances, R_{BL} and R_N, as follows:

$$R_{BL}/R_N = 1 + (N-1)(\tanh L)^2 + N \tanh (L) \sum_{k=1}^{M} 2^{(k-1)} \tanh (L - X_k). \quad (23)$$

This is the expression that was used to compute the table of illustrative values given in the Results section below; a more general expression is derived in the Appendix.

Steady-State Attenuation Factor from Branch Terminal to Soma

Attenuation factors are usually defined as the ratio of an amplitude or intensity at the input location to the smaller (attenuated) value found at a point of observation or output. So defined, the attenuation factor is a number greater than one; also, increased attenuation results in an increased attenuation factor. For the present problem of steady-state voltage attenuation, the voltage at the terminal of the input branch of the neuron model can be obtained most simply as

$$V_{BL} = IR_{BL}. \quad (24)$$

The corresponding voltage at the origin (soma) can be obtained by setting $X = 0$ in Eq. 12, 13, or 20; this gives

$$\begin{aligned} V_O &= IR_{T\infty}/(N \sinh L) \\ &= IR_N/\cosh L, \end{aligned} \quad (25)$$

where the second expression makes use of Eq. 11 for R_N.

Now, by taking the ratio of V_{BL} to V_O, we can write the following expression for the attenuation factor, from input branch terminal to the soma,

$$AF_{BL/O} = (R_{BL}/R_N) \cosh L, \tag{26}$$

where the ratio of input resistances inside the parentheses is precisely that defined by Eq. 23, above. This tells us that the attenuation factor is closely related to, but not identical with, the ratio of the input resistances at the input branch terminal and at the soma; the attenuation factor is always larger, because cosh (L) is greater than unity for all L values greater than zero. Illustrative values are given in the Results section, below; a more general expression is derived in the Appendix.

Note on Generalization of Theory

The Appendix provides more general results for branch input resistance and for attenuation factor. The input current can be applied at any point of any branch. Daughter branches need not be equal, but their diameters still must satisfy the more general equivalent cylinder constraint. Also, the dendritic trees need not be of equal trunk diameter, and the results are even further generalized to provide for trees that need not have the same electrotonic length. The final section of the Appendix provides results for AC steady-state impedance and attenuation.

ILLUSTRATIVE RESULTS

Example of Potential Distribution throughout Neuron Model

The method of solution described above has been used to compute the particular example illustrated in Fig. 4. This is a case of six dendritic trees with three orders of branching, i.e., $N = 6$ and $M = 3$. Here each tree has an electrotonic length $L = 1$ which is divided into four equal electrotonic increments, $\Delta X = 0.25$, for each trunk and each order of branching. The steepest gradient of membrane potential occurs in the input branch (BI); most of the input current reaches the parent branch point (P). Very little of this current flows out into the sister branch (BS); most of it flows through the parent branch where the gradient with respect to X is roughly half as steep as that in the input branch, because the R_∞ value of the parent branch cylinder is half that of the input branch cylinder. At the grandparent branch point (GP), relatively little current flows into the first cousin branches (BC-1), and most of the current flows through the grandparent branch, where the gradient with respect to X has been roughly halved again. In contrast to the steep gradients in the input branch and the parent and grandparent branches, the dashed curve in Fig. 4 shows the smaller gradient obtained if the same total amount of input currently were divided equally between the eight terminal branches of one dendritic tree. This dashed curve is continuous with the curve for this tree trunk; in fact, the solution in this trunk would be the same for any apportionment of the

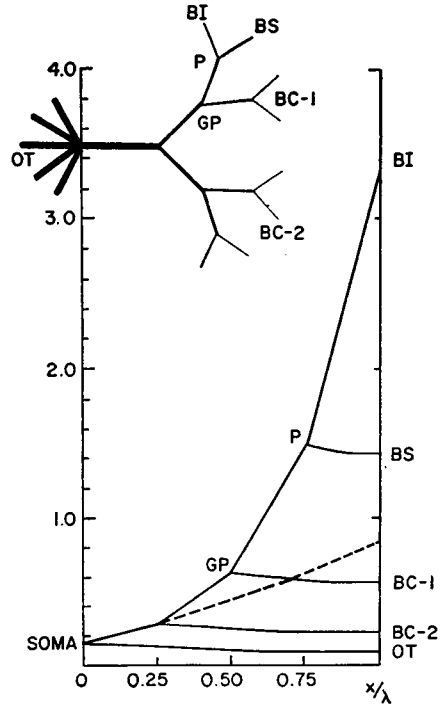

FIGURE 4 Branching diagram (upper left) and graph (below) showing steady-state values of V as a function of X in all branches and trees of the neuron model, for steady current injected into the terminal of one branch. BI and BS designate the input branch and its sister branch; P and GP designate their parent and grandparent branch points; BC-1 and BC-2 designate first and second cousin branches, with respect to the input branch; OT designates the other trees of the neuron model. The model parameters are $N = 6$, $L = 1$, $M = 3$, with equal electrotonic length increments $\Delta X = 0.25$ assumed for all branches. Ordinates of graph express V/IR_{T_∞} values, as defined by Eqs. 12, 13, and 20; see also expressions 27–31 and commentary in text.

same total input current between these eight branch terminals. Also, the solution from the soma into the five other trees (OT) is the same for any such apportionment of the same input.

The values of membrane potential shown in Fig. 4 are given as the dimensionless ratio of $V(X)$ to IR_{T_∞}. For the other trees (OT), these values were obtained from the expression

$$0.142 \cosh X - 0.108 \sinh X, \tag{27}$$

which follows from Eq. 13; (the minus sign is used here together with positive values of X for these cylinders). For the trunk of the input tree and for the dashed curve in Fig. 4, the values were obtained from the expression

$$0.142 \cosh X + 0.54 \sinh X, \tag{28}$$

which follows from Eq. 12. For the grandparent branch, which extends from $X = 0.25$ to $X = 0.5$, one must add to the value of expression 28, the value of

$$\sinh (X - 0.25)/\cosh (0.75), \tag{29}$$

based on Eq. 18. However, for the other half of this tree, extending from $X = 0.25$ to the four terminals of the second cousin branches (BC-2), the value of expression 29 was subtracted from that of expression 28.

For the parent branch, extending from $X = 0.5$ to $X = 0.75$, one must add to the value of expressions 28 plus 29 also the value of

$$2 \sinh (X - 0.5)/\cosh (0.5), \tag{30}$$

based on Eq. 19 with $k = 2$. For the input branch, extending from $X = 0.75$ to $X = 1.0$, one must add to the value of expressions 28 plus 29 and 30 also the expression

$$4 \sinh (X - 0.75)/\cosh (0.25), \tag{31}$$

based on Eq. 19 with $k = 3$. For the sister branch (BS), the value of expression 31 was subtracted from that of expressions 28 plus 29 and 30. In that portion of the tree which extends from the grandparent branch point (GP) to both terminals of the first cousin branches (BC-1), the value of expression 30 was subtracted from that of expressions 28 plus 29.

Examples of Input Resistance Ratio and Attenuation Factor

In Fig. 4, the value plotted for $V/IR_{T\infty}$ at the input terminal is about 3.4, while that at the origin (soma) is 0.142; the ratio of these two numbers gives a value of 23.9 for the attenuation factor from input terminal to soma. Alternatively, one can use Eq. 23 to obtain a value of 15.5 for the input resistance ratio R_{BL}/R_N, and then use Eq. 26 to obtain a value of 23.9 for the attenuation factor. Many additional examples have been calculated and listed in Table I.

All of the values in Table I depend upon specifying the values of N, L, and M for a symmetrically branched neuron model, with the additional simplifying assumption that the successive branch points X_k are equally spaced, with increments in X given by $\Delta X = L/(M + 1)$. The value inside each parenthesis in Table I gives the input resistance ratio R_{BL}/R_N, defined by Eq. 23. The value immediately below each parenthesis gives the corresponding attenuation factor, defined by Eq. 26. Several useful rough generalizations about the effects of changing the value of N, L, or M separately can be made from inspection of the values in Table I.

Effect of increasing L, with N and M constant. Consider the effect of doubling the value of L from 1.0 to 2.0; this means doubling all trunk and branch lengths, when expressed in units of X. Comparison of the first two columns of

TABLE I

INPUT RESISTANCE RATIO (R_{BL}/R_N) AND STEADY-STATE ATTENUATION FACTOR $AF_{BL/0}$

M	$N = 6$		$L = 1.5$	
	$L = 1.0$	$L = 2.0$	$N = 6$	$N = 10$
2	(9.5)	(17.4)	(14.3)	(23.6)
	14.7	65.5	33.6	55.4
3	(15.5)	(30.4)	(24.2)	(40.2)
	23.9	114	56.8	94.4
4	(26.0)	(53.6)	(41.7)	(69.4)
	40.1	202	98.0	163
5	(44.6)	(95.4)	(73.1)	(122)
	68.8	359	172	286
6	(78.0)	(172)	(130)	(216)
	120	647	305	508
7	(138)	(311)	(233)	(388)
	213	1170	548	912
8	(248)	(569)	(422)	(704)
	352	2140	992	1650

Table I shows that the input resistance ratio is roughly doubled, and that the attenuation factor increases roughly fivefold. With the larger M values, these factors of increase are somewhat larger.

Effect of increasing N, with L and M constant. We examine the effect of increasing N from 6 to 10, when $L = 1.5$ and M is constant, by comparing the last two columns of Table I. Both the input resistance ratio and the attenuation factor increase by a factor that is very close to 10/6. We can understand this most easily by considering, for example, that the dendritic trees are not changed in size (i.e., $R_{T\infty}$ is held constant). Then R_{BL} is little changed, because the distribution of input current in the input tree is almost unchanged; it is only slightly affected by the boundary condition (at the origin) with the other trees. However, the value of R_N is very significantly changed; the parallel input resistance of 10 trees must be reduced to exactly 6/10 of that for 6 trees of the same size. For such conditions, the increase in the input resistance ratio and in the attenuation factor can be attributed almost entirely to the 6/10 factor in R_N.

Effect of increasing M, with N and L constant. The previous example of $N = 6$, $L = 1$, and $M = 3$ implied trunk and branch increments of $\Delta X = 0.25$ (see Fig. 4). If we preserve these values of N and L, and increase M by four orders of branching to $M = 7$, this results in $\Delta X = 0.125$, with eight increments. The values in Table I show an approximately ninefold increase, from 15.5 to 138 for the input resistance ratio, and from 23.9 to 213 for the attenuation factor. Throughout Table I, an increase of M by four orders, while N and L are held constant, results in around a 9- or 10-fold increase. In other words, the factor of increase per

unit increase in M is given roughly by the square root of three, for the values in Table I. We gain some additional insight by noting that changes in M can have no effect upon the value of R_N when N, L, and $R_{T\infty}$ are held constant (see Eq. 11). Under such conditions, the increase in the input resistance ratio and in the attenuation factor, with increase in M, can be attributed entirely to the increase of R_{BL}, which can be attributed, in turn, to the smaller diameters of the higher order branches.

Nonreciprocity of Branch Attenuation

Comparison of the attenuation along the input branch and its sister branch (in Fig. 4) is instructive because neurophysiologists sometimes argue, erroneously, that the attenuation along a dendritic branch should be the same, whether it takes place in the centripetal or the centrifugal direction. This fallacy presumably results from noting that the core resistance is the same in both directions, while forgetting the importance of the boundary conditions. In Fig. 4, the attenuation from the parent branch point (P) to the terminal of the sister branch (BS) is rather small because of the insulated (zero slope) boundary condition at the terminal; in contrast, the attenuation from the terminal of the input branch (BI) to the pare nt branch point (P) is much larger because the boundary condition at P permits a large amount of current to flow from the input branch into the thicker parent branch. Here, the input branch and its sister branch have exactly the same core resistance; the difference results entirely from the boundary conditions. Similarly, in Fig. 2 the graphs show how attenuation from $X = L$ to the origin depends upon the boundary condition at the origin. An earlier publication (see Eq. 3 and Fig. 3, pp. 496–498, Rall, 1959) provides both a mathematical expression and a graphical illustration for such dependence of attenuation upon boundary conditions.

DISCUSSION

Application of Theoretical Results to Motoneurons

Motoneurons of cat spinal cord are large neurons whose input resistance values (R_N usually between 0.5 and 2.5 MΩ) are lower than for most other neurons in the mammalian central nervous system. The notion that the equivalent cylinder constraint might apply to motoneurons, at least as a rough approximation, was suggested some time ago (Rall, 1959) on the basis of preliminary evidence. Recently, Lux et al. (1970) checked 50 dendritic bifurcations in 7 carefully studied motoneurons and reported that the ratio of the summed $d^{3/2}$ of the daughter branches to the parent $d^{3/2}$ ranged from 0.8 to 1.2, with a mean of 1.02 ± 0.12 (SD). Also, Barrett and Crill (1971) found that (except for a sharp initial taper of the dendritic trunks) the summed $d^{3/2}$ value decreases only rather gradually with distance. These results, together with unpublished calculations based upon the data of Aitken and

Bridger (1961), imply that motoneuron dendritic trees may reasonably be approximated by equivalent cylinders, and furthermore, that the electrotonic length L for soma plus dendritic tree ranges between 1 and 2, with a mean value around 1.5 (see also Rall, 1964, 1969 *a*, 1970; Nelson and Lux, 1970; Burke and ten Bruggencate, 1971; Jack et al., 1970, 1971; Lux et al., 1970; Barrett and Crill, 1971). The study of Lux et al. (1970) is unusual in providing the first examples of estimation of L values by two independent methods on the same neuron; one method (Rall, 1959) depends upon anatomical measurements of branch lengths and diameters, together with the R_N measurement; the other method (Rall, 1969 *a*) is entirely electrophysiological, depending upon the theoretical relation between L and the time-constant ratio obtained by peeling the sum of exponential decays. Barrett and Crill (1971, plus personal communication) have recently also determined L by both methods on the same neuron.

Dendritic trees of different size occur on a single motoneuron. Also, the larger motoneurons tend to have both more numerous and larger dendritic trees than do the smaller motoneurons; see Kernell (1966), and also Gelfan et al. (1970). Such differences in tree size need not imply differences in electrotonic length L because the larger trunk diameters imply larger λ values. Thus, we have supposed that the separate L values of the separate dendritic trees belonging to a particular motoneuron could be nearly the same, in spite of differences in tree size. This supposition obtains support from the observation by Burke and ten Bruggencate (1971) that there is no significant correlation between whole motoneuron size (as indicated by R_N) and the L value estimated for the whole motoneuron; in other words, the observed range of L values was found to be the same for small motoneurons as for larger motoneurons. Because the large motoneurons possess more large dendritic trees, this result implies that the large dendritic trees do not have significantly larger L values. The measurements reported by Lux et al. (1970) and by Barrett and Crill (1971) also support this conclusion.

The early measurements of Coombs et al. (1955) and of Frank and Fuortes (1956) provided a range of cat motoneuron input resistance values of from 0.5 to 2.5 MΩ; this range was discussed in relation to dendritic anatomy by Rall (1959) and by Kernell (1966) and Burke (1967 *a*). Although these last two authors found a few larger R_N values, around 6–8 MΩ, most cat motoneuron input resistance values still lie in the original fivefold range. R_N values of 0.5 MΩ correspond to the largest motoneurons having the highest axonal conduction velocity and belong to fast twitch, phasic-type motor units; R_N values of 2–3 MΩ correspond to significantly smaller motoneurons having lower axonal conduction velocity and usually belonging to slow twitch, tonic-type motor units (Burke, 1967 *a*; cf., Wuerker et al., 1965; Kernell, 1966).

For this fivefold range in R_N, the terminal branch input resistance R_{BL} in a tree having about six or seven orders of branching, would be estimated in the range from roughly 40 to 350 MΩ for $L = 1.0$, and from roughly 65 to 750 MΩ for $L =$ 1.5–2.0, using Table I. For a dendritic tree with only three orders of branching, a

range of smaller values, roughly 7.5–75 MΩ for $L = 1.0$–2.0 would be estimated for R_{BL} ; however, so few orders of branching would be expected only in a small dendritic tree with small trunk diameter. For input to a midbranch ($X = L/2$) reference to the corresponding sections of the Appendix and Discussion suggest an input resistance roughly in the range from 1.5 to 20 MΩ, depending upon branch order.

Because we have specified branch order, but not branch diameter, in the examples above, it is useful to consider what branch diameters are implied by different orders of symmetric branching. For example, a tree with a trunk diameter of 5 μm and 7 orders of symmetric branching would imply a terminal branch diameter of 0.2 μm; a tree with a large trunk diameter of 20 μm would imply a 7th-order branch diameter of 0.8 μm, or a 10th-order branch diameter of 0.2 μm. These particular examples were chosen because 0.2 μm corresponds to the smallest terminal branch diameters observed by histologists (Golgi material and light microscopy by Dr. Aitken, personal communication; electron microscopy by Doctors Reese and White, personal communication).

With regard to steady-state voltage attenuation from a branch input site to a motoneuron soma, it is important to note the evidence that the dendritic membrane of cat motoneurons is normally passive. This is provided by the observation that whenever the combination of two excitatory postsynaptic potentials (EPSP) departs significantly from linearity, that departure has been a small deficit (Burke, 1967 *b*, pp. 1116–1120; Rall et al., 1967, pp. 1184–1185; see also Kuno and Miyahara, 1969). It is well known that such small deficits can be accounted for theoretically with the usual assumption that synaptic excitation consists of a conductance change in the postsynaptic membrane, where neither this synaptic conductance nor the adjacent passive membrane has voltage-dependent (regenerative) properties (Martin, 1955; Rall, 1967, p. 1157; Rall et al., 1967, p. 1183; Kuno, 1971; see also Eq. 32 below). On the other hand, if a small nonlinearity were caused by active membrane properties (local response), one would expect an excess (not a small deficit) of membrane depolarization; such small excess has not been reported for normal motoneurons. However, the abnormal "partial responses" of chromatolyzed motoneurons have been attributed to active properties of abnormal dendritic membrane, as contrasted with normally passive properties (Eccles et al., 1958; Kuno and Llinas, 1970). Thus, assuming normal membrane properties, our earlier example of a trunk diameter of 5 μm and a seventh-order terminal branch of 0.2 μm (with $N = 6$ and $L = 1.5$ in Table I) implies $R_{BL}/R_N = 233$ and a steady-state attenuation factor of 548. If this branch terminal were depolarized by 55 mV, the steady effect at the soma from this one steady input would be 0.1 mV.

Application to Other Neuron Types

Pioneering quantitative treatment of dendritic branching in cerebral cortex was provided by Bok (1936, 1959) and by Sholl (1953, 1956). The variety of dendritic

patterns in different neuron types has been emphasized and illustrated by Ramon-Moliner (1962, 1968) and by the Scheibels (1970). Improved quantitative methods were described and illustrated by Mannen (1966). The contributions of many other anatomists are reviewed in the papers cited above.

In order to apply the present theoretical results to any particular neuron type, one would like to have at least approximate answers to several questions. Does the dendritic branching approximately satisfy the equivalent cylinder constraint? Has an approximate range of R_N values been determined experimentally? Do the several dendritic trees seem to have similar electrotonic lengths, and, if so, has the range of such L values been estimated from experiment? Are estimates of N, M, and terminal branch diameter available? When the answers to these questions are affirmative, branch input resistance values can be estimated by means of the present theoretical results. If the branching does not satisfy the equivalent cylinder constraint, one must use the general method (Rall, 1959) for arbitrary branch lengths and diameters. For neurons where the evidence suggests active (nonlinear, regenerative) dendritic membrane properties, the attenuation factor expressions of the present paper do not apply.

Input resistance values have been measured for only a few types of neurons other than motoneurons; nearly all of these values have been larger, indicating that the neurons are smaller, and this accounts for the increased difficulty in obtaining reliable measurements with intracellular microelectrodes. Spencer and Kandel (1961) reported an average estimate of 13 MΩ for hippocampal neurons. Takahashi (1965) reported R_N values from 1.5 to 15 MΩ for pyramidal tract neurons, reporting a mean of 5.9 MΩ for 26 fast conducting cells and 10.1 MΩ for 10 slow conducting cells (see also Koike et al., 1968). Lux and Pollen (1966) obtained a range from 4.5 to 10 MΩ for identified Betz cells, and a wider range of 4.4–15.2 MΩ for nonidentified cortical cells (see also Creutzfeldt et al., 1964; Jacobson and Pollen, 1968). It seems reasonable to attribute R_N values around 4.5 MΩ to the larger pyramidal cells, and R_N values around 10–15 MΩ could be attributed to smaller pyramidal cells. Still larger R_N values would be expected for the smaller neurons of stellate and other cell types.

Calculations involving electrotonic distance in the apical dendrite of a pyramidal cell have been reported by Jacobson and Pollen (1968); see also Humphrey (1968) where emphasis was more upon extracellular potentials. Although the apical dendrite is usually much longer than the basilar dendrites, it is important to point out that this does not necessarily imply a larger L value, because the apical diameter is also larger. Furthermore, the well-known taper of apical dendritic diameter does not necessarily mean significant departure from the equivalent cylinder constraint, because the apical dendrite gives off side branches as it reduces its diameter. Jacobson and Pollen (1968) published a brief summary of their measurements and calculations based on a large sample of pyramidal cells. They mention seeing between 3 and 12 side branches of betwen 1 and 2 μm diameter along the major

stretch of the apical shaft; they also reported apical dendritic diameter at 50 μm intervals along a 250 μm length, both for the five largest pyramidal cells and for 80 small- and medium-sized pyramidal cells. It is interesting that the following examples, which are in general agreement with Jacobson and Pollen's data, also satisfy the equivalent cylinder constraint on $d^{3/2}$: a 2.2 μm apical diameter with a 1.0 μm side branch emerging from a 2.6 μm parent diameter; a 3.1 μm apical diameter with a 1.5 μm side branch emerging from a 3.8 μm parent diameter; a 4.6 μm apical diameter with a 2.0 μm side branch emerging from a 5.4 μm parent diameter. Because of the unequal branching, dendritic input resistances would be calculated by means of the general results in the Appendix. Also, with regard to electrotonic length estimation, we can use Jacobson and Pollen's apical diameters for the five largest pyramidal cells, plus their rough estimate of a 250 μm long secondary branch tapering from 2.5 to 2.0 μm diameter, and a 250 μm tertiary branch tapering from 2.0 to 1.5 μm. For the larger membrane resistivity (R_m = 4,500 Ω cm^2) we get ΔX values of about 0.3, 0.4, and 0.5 for these primary, secondary, and tertiary segments, giving a sum of about 1.2 for the apical value of L minus the still higher order branches; for the smaller R_m value of 1,500 Ω cm^2, the ΔX values are about 0.5, 0.7, and 0.8, giving a larger sum of about 2.0 for the apical value of L minus the still higher order branches. Unfortunately, we do not have the corresponding information on the basilar dendrites of these same cells. For several ranges of values, however, Jacobson and Pollen (1968) themselves obtained estimates of steady-state electrotonic attenuation over the apical dendritic length. Their results imply attenuation factors of about 3 or 4 from the major branch point (V_1) to soma, about 18 from the next branch point (V_2) to soma, and about 33–50 from the next branch point (V_3) to soma.

Local Synaptic Depolarization Not Proportional to Input Resistance

Because it is quite commonly believed that the amplitude of synaptic depolarization at the synaptic site should be expected to be directly proportional to the input resistance at that site, it seems important to draw attention to several reasons why such a strict proportionality should not be expected to hold, in general. It may be noted, however, that such proportionality can be a useful approximation for some situations; see, for example, Katz and Thesleff (1957), Katz and Miledi (1963), and Katz (1966); see also Kuno (1971), and MacGregor (1968).

First, it should be noted that brief synaptic input results in a transient EPSP, and even if the synaptic current generated at two different input sites were the same, the EPSP amplitude would depend not simply upon the input resistance at each site, but upon the different transient response function at each site. Furthermore, if there is significant depolarization of different amounts at the two synaptic sites, equal synaptic conductance transients would not produce equal synaptic current transients (Rall, 1967). Thus, in general, when comparing two synaptic sites, the

synaptic currents would be unequal, the transient response functions would not be related by any simple ratio, and the resulting peak depolarizations should not be expected to exhibit the input resistance ratio. The steady-state aspect of this problem is treated explicitly below; the transient details are included in the companion paper.[1] In any case, it is clear that when the effect of synaptic input to a fine dendritic branch having high input resistance is compared with that of equal synaptic input to a thicker branch having lower input resistance, the local depolarization (at the synaptic site) is larger at the site with the larger input resistance. This has led some (at least in conversation) to infer, erroneously, that such a larger local effect would produce a larger EPSP at the soma. The error here consists of forgetting that the attenuation from the synaptic site to the soma would be increased by a factor that is usually greater than the factor of input resistance increase (see Eq. 26); also, as noted already, the local depolarization at the synaptic site would be increased by a factor that is likely to be smaller than the factor of input resistance increase. The following example illustrates these two effects for a steady state; the overall discrepancy would be even greater for transients.

For a steady synaptic excitatory conductance g_e we can express the steady synaptic current as

$$(V_e - V_{in})g_e = V_{in}/R_{in}\,.$$

Where $V_e = E_e - E_r$ is the excitatory equilibrium potential, relative to the resting potential, and V_{in} is the resulting steady depolarization at the input site whose input resistance is R_{in}. Rearrangement of this expression provides the following useful expression for a single input,

$$(V_{in}/V_e) = (R_{in}g_e)/(1 + R_{in}g_e), \tag{32}$$

where it can be seen that steady V_{in} is proportional to $(R_{in}g_e)$ only when the value of $(R_{in}g_e)$ is much smaller than unity. Suppose, for example, that $g_e = 10^{-8}$ mho, and suppose, at the soma, $R_{in} = R_N = 10^6\ \Omega$; then Eq. 32 gives 0.01/1.01 for (V_{in}/V_e). Next, suppose we place the same steady-state synaptic conductance at a branch terminal, where, for example, $R_{in} = R_{BL} = 10^8\ \Omega$, or 100 times the previous input resistance; then Eq. 32 gives $(V_{in}/V_e) = 1/2$, which is 50 rather than 100 times the previous steady depolarization. To carry this example further, consider the attenuation from the branch terminal to the soma, and compare this attenuated amplitude with that found previously for input at the soma. In this example, $R_{BL}/R_N = 100$, and if we also assume $L = 1.5$, Eq. 26 implies an attenuation factor of 235; then the steady value of 1/2 for (V_{in}/V_e) at the input branch terminal implies a value of $(V/V_e) = 0.00212$ at the soma, or about one-fifth the value obtained when the same synaptic conductance was applied directly to the soma. To recapitulate this example, when the synaptic excitatory conductance was shifted from the soma to a branch terminal whose input resistance was 100

times as great as that at the soma, the steady depolarization at the synaptic site was increased 50 times, not 100 times; also, the steady attenuation factor of 235 from the input branch terminal to the soma resulted in a soma depolarization that was about one-fifth the reference value obtained with synaptic input at the soma.

Nonlinear Summation of Adjacent Dendritic Synaptic Inputs

It has already been pointed out elsewhere (Rall, 1967, pp. 1155–1156, 1167–1168; Rall et al., 1967, pp. 1183–1184) that the larger depolarization at a dendritic synaptic site can be responsible for significant nonlinearity of synaptic summation. This nonlinearity results because the depolarization due to one synapse reduces the synaptic driving potential ($V_s - V_{in}$) at the adjacent synapse;[8] the larger the local depolarization, the greater the nonlinear effect. In fact, we have argued that when an observed nonlinearity significantly exceeds the amount which could be accounted for by the depolarization at the soma, it is reasonable to suppose that the synaptic input sites must have been dendritic and sufficiently near each other for the depolarization produced by one to sufficiently reduce the effective synaptic driving potential of the other. Essentially the same concept has been used by Kuno and Miyahara (1969) to account for nonlinearities they observed. Also, MacGregor (1968) has recently stressed nonlinear effects in dendritic regions.

How Branch Input Resistance Differs from Core Resistance

It is of interest to examine the simple notion that branch input resistance might be estimated as the series resistance composed of R_N plus successive core resistance along the direct line from the input branch terminal to the soma. Such a resistance estimate can be shown mathematically (see below) to exceed the correct value of R_{BL}; a large discrepancy results with large electrotonic branch lengths, while smaller discrepancies result with small L and short electrotonic branch lengths. The physical intuitive explanation is that simple core resistance neglects the spread of current into the sister and cousin branches, and it also neglects the leakage of current across the dendritic membrane surface; in other words, it neglects the branching and cable properties of the dendrites. However, when a branch is short, little current leaks across its membrane, and consequently, the gradient of potential along its core is nearly constant; this can be seen in Fig. 4, where the slopes along the main line are nearly constant, and the slopes in the sister and cousin branches are rather small because they must be zero at their terminals. In this particular case, the series resistance estimate is 3.97 times $R_{T\infty}$, which is about 17% larger than the correct value of R_{BL}. A larger discrepancy results when we double L from 1.0 to 2.0, keeping $N = 6$ and $M = 3$. Then the series resistance estimate is 7.67 times $R_{T\infty}$, which is about 46% larger than the correct value of R_{BL}.

[8] In particular, if n equal synapses are active in very close proximity, we can replace g_s by the product ng_s in Eq. 32 to obtain the resultant local depolarizing effect.

To explain these results, we note first that for a length, $\Delta X = \Delta x/\lambda$, of a cylinder characterized by $R_\infty = \lambda r_i$, the core resistance can be expressed $r_i \Delta x = R_\infty(\Delta x/\lambda) = R_\infty \Delta X$. Thus, the core resistance of a kth order branch segment, extending from $X = X_k$ to $X = X_{k+1}$ of the neuron model, can be expressed as

$$2^k R_{T\infty}(X_{k+1} - X_k).$$

The proposition we wish to prove can be expressed

$$R_{BL} < R_N + R_{T\infty}\left\{X_1 + \sum_{k=1}^{M} 2^k(X_{k+1} - X_k)\right\}, \tag{33}$$

where the right side of this inequality represents the series resistance estimate composed of R_N plus successive core resistance segments along the direct route from the input branch terminal to the origin (soma).

In order to prove this inequality, we refer to Eq. 22 for R_{BL} and note a useful property of the hyperbolic tangent: although tanh (x) approximately equals x when x is small, it is always less than x; in fact, the first two terms of the series expansion (for values of x less than unity) give that tanh $(x) = x - x^3/3$. Thus, we can examine each term of the summation in Eq. 22 and express a corresponding inequality. We do this here for $k = M$, $k = M - 1, \ldots, k = 1$, and for the term in tanh (L):

$$2^{(M-1)} \tanh (L - X_M) < (L - X_M)2^{(M-1)}, \tag{34}$$

$$2^{(M-2)} \tanh (L - X_{M-1}) < (L - X_M)2^{(M-2)} + (X_M - X_{M-1})2^{(M-2)}, \tag{35}$$

$$\ldots \qquad \ldots \qquad \ldots$$

$$2^0 \tanh (L - X_1) < (L - X_M) + (X_M - X_{M-1}) + \ldots + (X_2 - X_1), \tag{36}$$

$$[(N - 1)/N] \tanh (L) < (L - X_M) + (X_M - X_{M-1}) + \ldots + (X_2 - X_1) + X_1. \tag{37}$$

It should be noted that the sum of the column composed of the first expression to the right of each inequality sign simplifies to $2^M(L - X_M)$; this times $R_{T\infty}$ is equal to the core resistance of the input branch. Furthermore, the sum of all the right-hand terms of inequalities 34–37 yields the expression inside the brackets of previous inequality 33, and this times $R_{T\infty}$ is equal to the series core resistance along the direct route from the input branch terminal to the origin. Thus, referring again to Eq. 22, we can see that if we multiply the left and right sides of inequalities 34–37 by $R_{T\infty}$ and then add R_N (Eq. 11) to both the sum of the left sides and the sum of

the right sides of the above inequalities, the result is precisely the inequality 33 which we set out to prove.

This proof not only demonstrates that R_{BL} is always less than this series resistance estimate, it also provides a detailed breakdown into component inequalities which can be examined to see how much each contributes. This, as well as several other points, can be illustrated by reference to Table II.

Components of Input Resistance and of Core Resistance. In Table II, the first row corresponds to inequality 34 and five subsequent rows correspond to inequalities 35–37, for the particular case of $N = 6$, $L = 1.5$, and $M = 5$, with equal increments, $\Delta X = 0.25$, for all branches. Columns A and B display the component terms of $R_{BL}/R_{T\infty}$, as defined by Eq. 22. It can be seen that the highest order term (3.92) makes the largest contribution to the numerical result; also, it differs least from its corresponding term in column C, because the hyperbolic tangent has the smallest argument. The fact that the two highest order terms are nearly equal in column B, and exactly equal in column C, results from two simplifying assumptions: the assumption of equal electrotonic length for the input branch and its parent branch, and the assumption of equal daughter diameters that satisfy the equivalent cylinder constraint. Subsequent terms in column B become progressively smaller, as the power of 2 becomes smaller in column A. The smallest term, 0.184, in column B corresponds to $R_N/R_{T\infty}$; it must be included to obtain the correct total for $R_{BL}/R_{T\infty}$, as defined by Eq. 22. When this total, 13.46, is divided by the value of $R_N/R_{T\infty}$, we obtain a value of 73.1 for R_{BL}/R_N, in agreement with the value given earlier in Table I, for $L = 1.5$, $N = 6$, and $M = 5$.

The core resistance of a kth-order branch is $2^k R_{T\infty}\Delta X$, for equal electrotonic length increments ΔX; see explanation in the sentences preceding inequality 33. For the present example, the value of the core resistance divided by $R_{T\infty}$ is 8.0 for

TABLE II

COMPONENTS OF INPUT RESISTANCE AND CORE RESISTANCE

(Using inequalities 34–37 for $N = 6$, L = 1.5, $\Delta X = 0.25$)

A		B		C		D		E		F						
2^4 tanh (0.25)	=	3.92	<	4.0	=	4.										
2^3 tanh (0.50)	=	3.70	<	4.0	=	2.	+	2.								
2^2 tanh (0.75)	=	2.54	<	3.0	=	1.	+	1.	+	1.						
2^1 tanh (1.0)	=	1.52	<	2.0	=	½	+	½	+	½	+	½				
2^0 tanh (1.25)	=	0.85	<	1.25	=	¼	+	¼	+	¼	+	¼	+	¼		
(5/6) tanh (1.5)	=	0.75	<	1.50	=	¼	+	¼	+	¼	+	¼	+	¼	+	¼
		13.28	<	15.75	=	8.	+	4.	+	2.	+	1.	+	½	+	¼
		+		+												
(1/6) coth (1.5)	=	0.184	=	0.184	= $R_N/R_{T\infty}$											
$R_{BL}/R_{T\infty}$	=	13.46	<	15.93	= $(R_N + R_{CORE})/R_{T\infty}$											

the input branch, 4.0 for its parent branch, and 2.0 for its grandparent branch. These values are to be found in Table II as the following column sums: sum of column D for the input branch, sum of column E for the parent branch, and sum of column F for the grandparent branch. Furthermore, the sum of all terms of the right-hand side of inequalities 34–37 provides the value 15.75 for the series core resistance divided by $R_{T\infty}$ along the direct route from the input terminal to the origin. By adding $R_N/R_{T\infty} = 0.184$ to this value, we obtain 15.93 for the right-hand side of inequality 33 divided by $R_{T\infty}$. This result exceeds the branch input resistance value, $R_{BL}/R_{T\infty} = 13.46$, by more than 18%. Even larger discrepancies result with larger values for L.

Effect of a Middendritic Input Location

Up to this point of the paper, we have considered only the input site at a dendritic terminal. What is the effect of shifting the input site to a middendritic location? One can guess, immediately, that the input resistance should be smaller than at the terminal for two reasons: the input branch diameter is larger, and the input current splits immediately into centripetal and centrifugal components. The exact mathematical consequences are derived in the Appendix; comparison of Eq. A 8 with Eq. 22 shows several changes. If the input site is at $X = X_i$ on a branch of order $k = k_i$, Eq. A 8 has X_i in place of L in the arguments of the numerators, and the summation runs only to $k = k_i$ instead of $k = M$; also, there is a factor, $\cosh(L - X_i)$ present. Suppose, for example, that $X_i = 0.5$ is used with $N = 6$, $L = 1.0$, and $M = 3$, or $M = 7$. This input site is exactly middendritic in terms of electrotonic distance. For $M = 3$, Eq. A 8 gives

$$R_{BX}/R_{T\infty} = (1.13)(0.16 + 0.28 + 0.20) = 0.72,$$

which is about 21% of the value (3.40) obtained for a terminal input site. For $M = 7$, Eq. A 8 gives $(1.13)(0.16 + 0.28 + 0.27 + 0.39 + 0.42)$ or 1.72 for $R_{BX}/R_{T\infty}$, which is only about 6% of the value (30.3) obtained for a terminal input site.

Effect of Unequal Branching

All of the results, so far, have been based upon the assumption of symmetric bifurcations along the input portion of the input tree; this makes the R_∞ value of the terminal branch cylinder equal to exactly $2^M R_{T\infty}$. However, it is important to note that these results have not depended upon symmetric branching in the other portions of the input tree, or in the other trees of the neuron model; this other branching can be profuse or sparse in terms of the number of orders M, and it can be asymmetric, provided that the equivalent cylinder constraint is satisfied, and that all terminals correspond to the same electrotonic distance $X = L$ from the origin. This generality holds because the equivalent cylinder for the (noninput) sister branch is all that enters into each superposition along the input branch lineage.

What, however, is the effect of asymmetric bifuractions along the input branch lineage? The solution to this problem is derived in the Appendix. Briefly, the R_∞ value of the input branch becomes generalized from $2^M R_{T\infty}$ to the product, $\gamma_1\gamma_2 \ldots \gamma_M R_{T\infty}$, where each of these γ_k is the ratio of the R_∞ of the input carrying daughter cylinder at the kth branch point, to the R_∞ of its parent cylinder. For symmetric branching, each γ_k would equal 2; when the input carrying daughter cylinder is thinner than its sister branch, γ_k is greater than 2. In the expression for R_{BL}, the factor, $2^{(k-1)}$ in the summation expression becomes replaced by a product, $\gamma_1\gamma_2 \ldots (\gamma_k - 1)$; compare Eq. A 9 with earlier Eq 20. Clearly, if all of the γ_k are greater than 2, both R_{BL} and the R_∞ value of the terminal branch cylinder would be greater than for the case of symmetric bifurcations; also, the attenuation factor would be greater. On the other hand, for randomized asymmetries where γ_k values less than 2 are as probable as values greater than 2, these effects will tend to cancel. Any specific example can be computed in detail.

Effect of Unequal Trees

Although the body of this paper presents a model composed of equal dendritic trees, the superposition method can be generalized to treat unequal trees. It is simplest to consider different trunk diameters while preserving a common electrotonic length L for all trees. However, Eqs. A 9–A 12 of the Appendix show how unequal L values can also be provided for. These expressions involve the ratio γ which equals the ratio of the combined input conductance of all dendritic trees (from their common origin) to the input conductance of the input tree alone. Each tree must still have branch diameters that satisfy the equivalent cylinder constraint, but the N equivalent cylinders can now have different lengths and diameters. If these lengths and diameters are all made equal, the ratio γ reduces to N.

SUMMARY

(*a*) Mathematical solutions and numerical illustrations are presented for the steady-state distribution of membrane potential in an extensively branched neuron model, when steady electric current is injected into only one dendritic branch. The model assumes that the dendritic membrane is passive and that the dendritic trees satisfy the equivalent cylinder constraint on branch diameters. Although the initial derivation assumes equal dendritic trees and symmetric dendritic branching, these simplifying assumptions are dispensed with in the Appendix. Also, the initial derivation limits the site of current injection to the end of a terminal branch, while the generalization in the Appendix permits the input site to be located anywhere on any branch or trunk of a dendritic tree.

(*b*) These solutions provide us with explicit expressions for input resistance at a branch input site, and for the attenuation factor for voltage attenuation from the input site to the soma. It is useful to express the branch input resistance relative to

the whole neuron resistance R_N measured at the soma (origin) of the model. The attenuation factor is related to, but always greater than, this input resistance ratio.

(*c*) Table I illustrates many numerical examples of this input resistance ratio and the attenuation factor, for the case of symmetric branching, with equal electrotonic increments per branch, and with input injected at a branch terminal; the input resistance ratios range from about 10 to 700, while the attenuation factors range from about 15 to 2,000, for the ranges of N, L, and M assumed for this table. Increasing the number of orders of branching M, while keeping the number of trees N and their electrotonic length L constant, increases both the input resistance ratio and the attenuation factor approximately threefold for a two unit increase in M. Increasing N, while L and M are held constant, increases both the input resistance ratio and the attenuation factor in nearly direct proportionality with the increase in N. Doubling L from 1.0 to 2.0, with N and M held constant, approximately doubles the input resistance ratio, and increases the attenuation factor about fivefold.

(*d*) The application to cat spinal motoneurons is discussed with attention to recent experimental evidence showing that these neurons satisfy the various assumptions of the model to at least a reasonable approximation. Terminal branch input resistance values are estimated to lie in the range from roughly 40 to 750 MΩ; for middendritic input sites the range would be smaller, roughly 1.5–20 MΩ, or more for high orders of middendritic branching.

(e) Although applicability of the theory to other neurons is handicapped by insufficient information, the requirements are discussed and the case of pyramidal tract neurons is reviewed.

(*f*) The theoretical solution in the dendritic trunk (and at the soma) is the same whether injected current is applied entirely to one branch or is divided between several branches of the same tree, provided that the injection sites are all at the same electrotonic distance from the soma. This does not hold for input as a synaptic membrane conductance.

(*g*) Membrane depolarization at the site of a steady synaptic conductance input is not, in general, directly proportional to the input resistance. While a high input resistance does yield a larger local depolarization, this depolarization itself causes a deficit in synaptic current, because it decreases the effective synaptic driving potential. Also, because of increased electrotonic attenuation, the large depolarization at a dendritic synaptic site yields less soma depolarization than if the same synaptic conductance input were delivered directly to the soma.

(*h*) It is shown that branch input resistance exceeds the input resistance at the soma by an amount that is always less than the series sum of core resistances along the path from the input site to the soma.

(*i*) Several significant generalizations of the theoretical results are provided in the Appendix: the dendritic trees can be unequal in trunk diameter and in electrotonic length; daughter branch diameters can be unequal but must satisfy the equiv-

alent cylinder constraint; the site of current injection can be anywhere on a branch of any order.

(*j*) Expressions are also derived for input impedances and attenuation for AC steady states.

APPENDIX

More General Theoretical Results

Additional Symbols Used in Appendix

X_i	Electrotonic distance from the origin to the point of current *injection*, not restricted to $X = L$.
V_i	Value of V at the point of current *injection*.
$R_{G,\,\mathrm{ins}}(X_i, L, R_\infty)$	Input resistance at the point ($X = X_i$) in a *cylinder insulated* ($dV/dX = 0$) at the origin as well as at $X = L$; Eq. A 1.
$R_{G,\,\mathrm{clp}}(X_i, L, R_\infty)$	Input resistance at the point ($X = X_i$) in a *cylinder clamped* ($V = 0$) at the origin, but insulated at $X = L$; Eq. A 2.
$R_{NG}(X_i, L, N, R_{T\infty})$	Input resistance at the point ($X = X_i$) of one equivalent *cylinder* of the *neuron* model; or parallel input resistance of all branches (at $X = X_i$) belonging to one dendritic tree of the neuron model; Eq. A 5.
k_i	Branching order of the one branch which receives input at $X = X_i$.
R_{BX}	Input resistance at the point ($X = X_i$) on one dendritic *branch* of order (k_i); function of ($X_i, k_i, L, N, R_{T\infty}$) with symmetric branching; Eq. A 8.
R_B	More general *branch* input resistance at the point ($X = X_i$) for nonsymmetric branching and unequal trees (branching must still satisfy equivalent cylinder constraint); see Eq. A 11.
γ	Ratio of combined input conductance of all dendritic trees (at their common origin) to the input conductance of the input tree; Eq. A 10; reduces to N for equal trees.
γ_1	Ratio of the $d^{3/2}$ value for the trunk of the input tree to the $d^{3/2}$ value for the first-order branch which leads to the input site.
γ_k	Ratio at kth-order branch point of the parent $d^{3/2}$ value to the $d^{3/2}$ value of the input carrying daughter branch.
p_k	Product which reduces to $2^{(k-1)}$ for symmetric branching; see Eqs. A 9–A 12.
$AF_{BX/O}$	General attenuation factor from $X = X_i$ to soma; Eq. A 12.
$\omega = 2\pi f$	Angular frequency for a sinusoidal steady state.
$j = (-1)^{1/2}$	For complex variable notation.
$q = (1 + j\omega\tau)^{1/2} = (Y_m/G_m)^{1/2}$	Complex function of frequency; function of membrane admittance to conductance ratio.
$r = (1 + \omega^2\tau^2)^{1/2} = a^2 + b^2$	Modulus of q^2.
$a = [(r + 1)/2]^{1/2}$	Real part of q.
$b = [(r - 1)/2]^{1/2}$	Imaginary part of q.

$\alpha = 2aL$; $\alpha_k = 2a(L - X_k)$.
$\beta = 2bL$; $\beta_k = 2b(L - X_k)$.

$Z_{CL,\ \mathrm{ins}}$ — Input impedance at the end ($X = L$) for a *cylinder insulated* ($dV/dX = 0$) at the origin; Eq. A 15.

$Z_{CL,\ \mathrm{clp}}$ — Input impedance at the end ($X = L$) for a *cylinder clamped* ($V = 0$) at the origin; Eq. A 16.

Z_N — Whole *neuron* input impedance at the point ($X = 0$) of common origin of N equal dendritic trees or equivalent cylinders; Eq. A 17.

Z_{BL} — *Branch* input impedance at the end ($X = L$) of one terminal branch of the neuron model.

Effect of Input Site Not Restricted to $X = L$

When the point of current injection is located at the electrotonic distance, $X = X_i < L$, from the origin, the injected current divides into a centrifugal and a centripetal component. For a single cylinder of length $2L$ even symmetry (compare earlier Fig. 2 A and Eqs. 4–7) would require a source current of $I/2$ at $X = -X_i$ as well as $X = +X_i$. This even symmetry implies $dV/dX = 0$ at $X = 0$, and insulated ends also imply that $dV/dX = 0$ at $X = \pm L$. For positive values of X, we need to match solutions for the two regions that join at $X = X_i$. We can write

$$V(X) = V_i \cosh X/\cosh X_i, \quad \text{for } 0 \leq X \leq X_i,$$

and

$$V(X) = V_i \cosh (L - X)/\cosh (L - X_i), \quad \text{for } X_i \leq X \pm L.$$

which provide continuity of $V(X)$ at $X = X_i$, and which also satisfy $dV/dX = 0$ at $X = 0$ and $X = L$. In other words, these three boundary conditions have been used to determine three of four arbitrary constants; the remaining constant V_i must be determined from the requirement that $I/2$ equal the amount of core current flowing away from $X = X_i$. This can be expressed

$$I/2 = (V_i/R_\infty)[\tanh X_i + \tanh (L - X_i)]$$

$$= (V_i/R_\infty) \sinh L/[\cosh X_i \cosh (L - X_i)].$$

From this it follows that the input resistance, $V_i/(I/2)$, can be expressed

$$R_{C,\ \mathrm{ins}}(X_i, L, R_\infty) = R_\infty \cosh (L - X_i) \cosh X_i/\sinh L, \qquad (A\ 1)$$

for a cylinder of length L insulated at both $X = 0$ and $X = L$, with steady input current injected at $X = X_i$. This input resistance clearly depends upon three parameters, L, R_∞, and X_i. When $X_i = L$, this reduces to Eq. 7; it can be seen that $X_i = 0$ also gives the same result.

For the corresponding case of odd symmetry, with a source current $I/2$ at $X = X_i$, and a matching sink current $-I/2$ at $X = -X_i$ (compare earlier Fig. 2 B and Eqs. 8 and 9), similar treatment of this problem yields the input resistance

$$R_{C,\ \mathrm{clp}}(X_i, L, R_\infty) = R_\infty \cosh (L - X_i) \sinh X_i/\cosh L, \qquad (A\ 2)$$

for a cylinder of length L, which is clamped ($V = 0$) at $X = 0$, and insulated at $X = L$, with steady input current injected at X_i. This input resistance reduces to Eq. 9 when $X_i = L$.

By making use of the insight contained in earlier Eq. 15 and the physical interpretation given in the paragraph following it, the corresponding superposition for the present problem provides the solution for the injection of steady current I at the point $X = X_i$, in only one of N equal cylinders coupled at $X = 0$. For the range, $0 \leq X \leq X_i$ of the input cylinder, this solution can be expressed

$$V(X) = IR_{T\infty} \cosh (L - X_i) \left\{ \frac{\cosh X}{N \sinh L} + \frac{(N - 1) \sinh X}{N \cosh L} \right\}. \quad (A\,3)$$

At the origin, this simplifies to

$$\begin{aligned} V(O) &= (I/N)R_{T\infty} \cosh (L - X_i)/\sinh L \\ &= IR_N \cosh (L - X_i)/\cosh L, \end{aligned} \quad (A\,4)$$

where the second form makes use of Eq. 11 for R_N. This result remains unaffected by the branching considerations that follow; it is used later to obtain an expression for a generalized attenuation factor.

When we set $X = X_i$ in Eq. A 3, the result can be expressed $V(X_i) = IR_{NC}$, where R_{NC} represents the input resistance for this case. This input resistance can be expressed

$$R_{NC}(X_i, L, N, R_{T\infty}) = R_{T\infty} \cosh (L - X_i) \cdot \left\{ \frac{\cosh (X_i)}{N \sinh L} + \frac{(N - 1) \sinh (X_i)}{N \cosh L} \right\}, \quad (A\,5)$$

for current injection at $X = X_i$ to only one of N equal cylinders coupled at the origin. This input resistance reduces to Eq. 14 when $X_i = L$; it also reduces to Eq. 11 when $X_i = 0$.

Next, consider one order of symmetric dendritic branching, with $X_i > X_1$. Then the odd symmetry for $I/2$ applied at X_i of the input branch, with a matching $-I/2$ applied at X_i of the sister branch, is responsible for a contribution corresponding to Eq. 18 but modified as suggested by a comparison of Eq. A 2 with Eqs. 8 and 9. Here, this contribution can be expressed

$$V(X) = (I/2)(2R_{T\infty}) \cosh (L - X_i) \sinh (X - X_1)/\cosh (L - X_1), \quad (A\,6)$$

and a similar contribution is provided by each order of branching for which the branch point occurs at an electrotonic distance less than X_i from the origin. Let k_i represent the order of the branch which receives the input current. The solution in the input branch, for $X_{k_i} \leq X \leq X_i$, can be written as

$$V(X) = IR_{T\infty} \cosh (L - X_i) \cdot \left\{ \frac{\cosh X}{N \sinh L} + \frac{(N - 1) \sinh X}{N \cosh L} + \sum_{k=1}^{k_i} 2^{(k-1)} \frac{\sinh (X - X_k)}{\cosh (L - X_k)} \right\}, \quad (A\,7)$$

which differs from Eq. 20 (for input branch) in two respects: the factor $\cosh (L - X_i)$, and the fact that the summation runs to $k = k_i$ rather than to $k = M$. Clearly, Eq. A 7 reduces

to this earlier result when $X_i = L$, with $k_i = M$. By setting $X = X_i$ in Eq. A 7 and dividing by I, we obtain the corresponding expression for input resistance

$$R_{BX} = R_{T\infty} \cosh (L - X_i) \cdot \left\{ \frac{\cosh (X_i)}{N \sinh L} + \frac{(N-1) \sinh (X_i)}{N \cosh L} + \sum_{k=1}^{k_i} 2^{(k-1)} \frac{\sinh (X_i - X_k)}{\cosh (L - X_k)} \right\}, \quad (A\,8)$$

which may be compared with previous Eq. 22.

Effects of Unequal Trunks and Branches

There is no difficulty in treating trunks and branches of unequal diameter, provided that all of the trees satisfy the equivalent cylinder constraint (preservation of $\sum d^{3/2}$ with successive branching). This is simplest when these trees all have the same electrotonic length L. In our derivation, the importance of N was that it represented the ratio of the summed $d^{3/2}$ value (for all trunks of the neuron model) to the $d^{3/2}$ value of the trunk of the input tree, alone; when the trunk diameters are unequal, this ratio of $d^{3/2}$ values can be designated[9] as γ. Then, also the ratio of the $d^{3/2}$ sum for the "other" cylinders to that for all cylinders can be expressed as $(\gamma - 1)/\gamma$, corresponding to $(N - 1)/N$ of the previous derivations.

Similarly, for first-order branches of unequal diameter, we use γ_1 to designate the ratio of trunk $d^{3/2}$ to the $d^{3/2}$ value of the input receiving branch. The equivalent cylinder constraint implies that the corresponding ratio for the sister branch is $\gamma_1/(\gamma_1 - 1)$ because the reciprocal of this plus the reciprocal of γ_1 must sum to unity. Referring to Fig. 3 A, but with unequal branch diameters, we can see that the input current would not be represented as two equal source currents of $I/2$, but rather, a source current of I/γ_1 in the input branch, together with a different source current of $(\gamma_1 - 1)I/\gamma_1$ in the sister branch. Then, the source-sink pair of Fig. 3 B must be chosen to be currents of plus and minus$(\gamma_1 - 1)I/\gamma_1$, in order to obtain a zero slope at the sister terminal after superposition, corresponding to Fig. 3 C. This means that the product, $(I/2)$ times $(2R_{T\infty})$, in Eq. 18 or A 6 for the source branch of the previous derivation, must be replaced by the product, $(\gamma_1 - 1)I/\gamma_1$ times $(\gamma_1 R_{T\infty})$, which equals $(\gamma_1 - 1)IR_{T\infty}$; it should be noted that $\gamma_1 R_{T\infty}$ is the R_∞ value of this branch cylinder. Superposition of this source-sink current with the source current of I/γ_1 in the input branch results in a total source current of I in the input branch. Thus, with the next order of branching, we are led to a source-sink current of $(\gamma_2 - 1)I/\gamma_2$ multiplied by a R_∞ value of $\gamma_1\gamma_2 R_{T\infty}$ for the input branch; this product equals $\gamma_1(\gamma_2 - 1)IR_{T\infty}$. With kth-order branching, this product becomes $\gamma_1\gamma_2 \ldots (\gamma_k - 1)IR_{T\infty}$ instead of the product, $(I/2)(2^k R_{T\infty}) = 2^{(k-1)} IR_{T\infty}$ of previous Eq. 19.

Now, referring to Eqs. 20 and A 7, we are ready to write the generalized expression for the distribution of steady potential in the input branch, allowing both for X_i different from L and for unequal trunk and branch diameters. This result can be expressed,

$$V(X) = IR_{T\infty} \cosh (L - X_i) \cdot \left\{ \frac{\cosh X}{\gamma \sinh L} + \frac{(\gamma - 1) \sinh X}{\gamma \cosh L} + \sum_{k=1}^{k_i} p_k \frac{\sinh (X - X_k)}{\cosh (L - X_k)} \right\}, \quad (A\,9)$$

[9] The ratio γ takes the more general form shown below in Eq. A 10 when dendritic trees can have unequal L values as well as unequal diameters.

where $p_1 = (\gamma_1 - 1)$, $p_2 = \gamma_1(\gamma_2 - 1), \ldots p_k = \gamma_1\gamma_2 \ldots (\gamma_k - 1)$, with γ_1, $\gamma_2 \ldots \gamma_k$ defined as in the preceding paragraph, and where γ is defined by Eq. A 10 below; also, $R_{T\infty}$ and L refer here specifically to the input receiving tree.

Effect of Including Trees with Unequal L Values. In order to find the effect of unequal L values, we refer to the analysis associated with Figs. 2 D, E, F and Eqs. 12–15, where the superposition of unbranched cylinders was presented. There the component source currents and sink currents were all of equal magnitude; here these component currents must be chosen unequal in order to obtain the required superposition result. Corresponding to the even-type symmetries of Fig. 2 D, we choose unequal source currents which satisfy the previous condition at the origin, namely, $dV/dX = 0$ with a common value of V. Then, corresponding to the odd-type symmetries of Fig. 2 E, we choose unequal source-sink combinations which satisfy the following conditions: each sink current (cf., Fig. 2 E) is chosen to cancel exactly the source current (cf., Fig. 2 D) at the terminal of one of the $(N - 1)$ other cylinders; also, at the origin, $V = 0$ and the current is continuous. The result of the complete superposition is to find that γ, in Eq. A 9, represents the following generalized ratio,

$$\gamma = \left(\sum_j d_j^{3/2} \tanh L_j\right) / (d_i^{3/2} \tanh L_i), \tag{A 10}$$

where d_i and L_i refer to the input receiving cylinder, and where the summation is taken over all N cylinders, including the input cylinder. This ratio has a simple physical interpretation: it is the ratio of the combined input conductance of all cylinders (from their common origin) to the input conductance of the input cylinder alone (taken from this origin). When all L_j are equal, γ reduces to the $d^{3/2}$ ratio noted earlier, and when all d_j are also equal, $\gamma = N$.

More General Input Resistance Ratio and Attenuation Factor

We can now obtain a more general input resistance R_B by setting $X = X_i$ in Eq. A 9, and dividing by the input current I. If we also note that Eq. 11 for R_N should be generalized by replacing N with γ, we can write our general result as the input resistance ratio,

$$\frac{R_B}{R_N} = \cosh (L - X_i) \left\{\frac{\cosh (X_i)}{\cosh L} + \frac{(\gamma - 1) \sinh (X_i)}{(\coth L)(\cosh L)} + \frac{\gamma}{\coth L} \sum_{k=1}^{k_i} p_k \frac{\sinh (X_i - X_k)}{\cosh (L - X_k)}\right\}. \tag{A 11}$$

Also, the more general attenuation factor can be expressed in two useful forms,

$$\begin{aligned} AF_{BX/O} &= (R_B/R_N)(\cosh L)/\cosh (L - X_i) \\ &= \cosh (X_i) + \frac{(\gamma - 1) \sinh (X_i)}{\coth L} \\ &\quad + \gamma \sinh L \sum_{k=1}^{k_i} p_k \frac{\sinh (X_i - X_k)}{\cosh (L - X_k)}. \end{aligned} \tag{A 12}$$

It can be seen that when $X_i = L$, $\gamma = N$, and $p_k = 2^{(k-1)}$, Eqs. A 11 and A 12 reduce to previous Eqs. 23 and 26.

Generalization to AC Steady-State Impedance and Attenuation

The same superposition scheme can be used for the AC steady state. Current and voltage become complex quantities; conductances and resistances are replaced by complex admittances and impedances. For a sinusoidal angular frequency, $\omega = 2\pi f$, the ratio of membrane admittance per unit area to membrane conductance per unit area can be expressed,

$$Y_m/G_m = 1 + j\omega\tau = q^2.$$

The cable equation for AC steady states in nerve cylinders can be expressed

$$d^2V/dX^2 - q^2V = 0, \tag{A 13}$$

which may be compared with Eq. 1 of the earlier derivation. The corresponding general solution can be expressed

$$V(X, \omega) = A \sinh (qX) + B \cosh (qX), \tag{A 14}$$

where we note that differentiation with respect to X will introduce the complex factor q into the expressions for slope and for core current.

Following the previous consideration of the even and odd symmetries in Figs. 2 A and 2 B, we obtain the corresponding impedances,

$$Z_{CL,\text{ins}} = (R_\infty/q) \coth (qL), \tag{A 15}$$

and

$$Z_{CL,\text{clp}} = (R_\infty/q) \tanh (qL). \tag{A 16}$$

It may be noted that for zero frequency, $q = 1$, and these impedances reduce to the corresponding resistances of Eqs. 7 and 9.

In the same way, the whole neuron impedance at the origin of the model with N equivalent cylinders or trees, can be expressed

$$\begin{aligned} Z_N &= (R_{T\infty}/qN) \coth (qL) \\ &= (R_N/q) \tanh L \coth (qL). \end{aligned} \tag{A 17}$$

Also, by noting previous Eqs. 14 and 15 together with Eqs. 22 and 23, we can write down the corresponding expression for the ratio of branch terminal input impedance to Z_N, as follows

$$\begin{aligned} Z_{BL}/Z_N = 1 &+ (N - 1)[\tanh (qL)]^2 \\ &+ N \tanh (qL) \sum_{k=1}^{M} 2^{(k-1)} \tanh [q(L - X_k)]. \end{aligned} \tag{A 18}$$

Similarly, the attenuation factor from the input terminal to the origin (soma) of the model can be expressed as the modulus of V_{BL}/V_O, as follows

$$| V_{BL}/V_O | = | Z_{BL}/Z_N \| \cosh (qL) |. \tag{A 19}$$

In order to obtain the real and imaginary parts of these complex impedances and ratios, we make use of the definitions of a, b, and r (see list at beginning of Appendix) as the real part, imaginary part, and the squared modulus, respectively, of q, together with the following two identities:

$$\tanh(qL) = (\sinh \alpha + j \sin \beta)/(\cosh \alpha + \cos \beta),$$

$$\coth(qL) = (\sinh \alpha - j \sin \beta)/(\cosh \alpha - \cos \beta),$$

where $\alpha = 2aL$, and $\beta = 2bL$. Making use of these definitions and identities, we can express the real and imaginary parts of Z_N as

$$\Re(Z_N) = \frac{R_N(\tanh L)(a \sinh \alpha - b \sin \beta)}{r(\cosh \alpha - \cos \beta)},$$

$$\Im(Z_N) = \frac{R_N(\tanh L)(-b \sinh \alpha - a \sin \beta)}{r(\cosh \alpha - \cos \beta)},$$

and the modulus can be expressed as

$$|Z_N| = \frac{R_N(\tanh L)(\sinh^2 \alpha + \sin^2 \beta)^{1/2}}{(r)^{1/2}(\cosh \alpha - \cos \beta)}.$$

Also, the ratio of the imaginary to the real part provides the tangent of the phase angle.

A similar treatment of the impedance ratio Z_{BL}/Z_N can be carried out, where we also define $\alpha_k = 2a(L - X_k)$ and $\beta_k = 2b(L - X_k)$. Then

$$\Re(Z_{BL}/Z_N) = 1 + \frac{(N-1)(\sinh^2 \alpha - \sin^2 \beta)}{(\cosh \alpha + \cos \beta)^2} + N \sum_{k=1}^{M} 2^{(k-1)} \left[\frac{\sinh \alpha \sinh \alpha_k - \sin \beta \sin \beta_k}{(\cosh \alpha + \cos \beta)(\cosh \alpha_k + \cos \beta_k)} \right],$$

$$\Im(Z_{BL}/Z_N) = \frac{(N-1)(2 \sinh \alpha \sin \beta)}{(\cosh \alpha + \cos \beta)^2} + N \sum_{k=1}^{M} 2^{(k-1)} \left[\frac{\sinh \alpha \sin \beta_k + \sinh \alpha_k \sin \beta}{(\cosh \alpha + \cos \beta)(\cosh \alpha_k + \cos \beta_k)} \right].$$

These results can then be used to compute the modulus, $|Z_{BL}/Z_N|$, and then the AC attenuation factor defined by Eq. A 19.

Received for publication 30 November 1972.

REFERENCES

AITKEN, J., and J. BRIDGER. 1961. *J. Anat.* **95**:38.

ARSHAVSKII, Y. I., M. B. BERKINBLIT, S. A. KOVALEV, V. V. SMOLYANINOV, and L. M. CHAILAKHYAN. 1965. *Dokl. Biophys.* **163**:994.

BARRETT, J. N., and W. E. CRILL. 1971. *Brain Res.* **28**:556.

BOK, S. T. 1936. *Proc. K. Ned. Akad. Wet. Ser. B Phys. Sci.* **39**:1209.

BOK, S. T. 1959. *Histonomy of the Cerebral Cortex. Elsevier, Amsterdam.*
BURKE, R. E. 1967 *a. J. Physiol. (Lond.).* **193**:141.
BURKE, R. E. 1967 *b. J. Neurophysiol.* **30**:1114.
BURKE, R. E., and G. TEN BRUGGENCATE. 1971. *J. Physiol. (Lond.).* **212**:1.
COOMBS, J. S., J. C. ECCLES, and P. FATT. 1955. *J. Physiol. (Lond.).* **130**:291.
CREUTZFELDT, O. D., H. D. LUX, and A. C. NACIMENTO. 1964. *Pflügers Arch. Gesamte Physiol. Menscher Tiere.* **281**:129.
ECCLES, J. C., B. LIBET, and R. R. YOUNG. 1958. *J. Physiol. (Lond.).* **143**:11.
FRANK, K., and M. G. F. FUORTES. 1956. *J. Physiol. (Lond.).* **134**:451.
GELFAN, S., G. KAO, and D. S. RUCHKIN. 1970. *J. Comp. Neurol.* **139**:385.
HUMPHREY, D. R. 1968. *Electroencephalogr. Clin. Neurophysiol.* **25**:421.
JACK, J. J. B., S. MILLER, R. PORTER, and S. J. REDMAN. 1970. *In* Excitatory Synaptic Mechanisms. P. Andersen, and J. K. S. Jansen, editors. Universitets Forlaget, Oslo. 199.
JACK, J. J. B., S. MILLER, R. PORTER, and S. J. REDMAN. 1971. *J. Physiol. (Lond.).* **215**:353.
JACK, J. J. B., and S. J. REDMAN. 1971. *J. Physiol. (Lond.).* **215**:321.
JACOBSON, S., and D. A. POLLEN. 1968. *Science (Wash. D. C.).* **161**:1351.
KATZ, B. 1966. Nerve, Muscle and Synapse. McGraw-Hill Book Company, New York.
KATZ, B., and R. MILEDI. 1963. *J. Physiol. (Lond.).* **168**:389.
KATZ, B., and S. THESLEFF. 1957. *J. Physiol. (Lond.).* **137**:267.
KERNELL, D. 1966. *Science (Wash. D. C.).* **152**:1637.
KOIKE, H., Y. OKADA, T. OSHIMA, and K. TAKAHASHI. 1968. *Exp. Brain Res.* **5**:173.
KUNO, M. 1971. *Physiol. Rev.* **51**:657.
KUNO, M., and R. LLINAS. 1970. *J. Physiol. (Lond.).* **210**:807.
KUNO, M., and J. T. MIYAHARA. 1969. *J. Physiol. (Lond.).* **201**:465.
LUX, H. D., and D. A. POLLEN. 1966. *J. Neurophysiol.* **29**:207.
LUX, H. D., P. SCHUBERT, and G. W. KREUTZBERG. 1970. *In* Excitatory Synaptic Mechanisms. P. Andersen, and J. K. S. Jansen, editors. Universitets Forlaget, Oslo. 189.
MACGREGOR, R. J. 1968. *Biophys. J.* **8**:305.
MANNEN, H. 1966. *Prog. Brain Res.* **21A**:131.
MARTIN, A. R. 1955. *J. Physiol. (Lond.).* **130**:114.
NELSON, P. G., and H. D. LUX. 1970. *Biophys. J.* **10**:55.
RALL, W. 1959. *Exp. Neurol.* **1**:491.
RALL, W. 1960. *Exp. Neurol.* **2**:503.
RALL, W. 1962. *Ann. N. Y. Acad. Sci.* **96**:1071.
RALL, W. 1964. *In* Neural Theory and Modeling. R. F. Reiss, editor. Stanford University Press, Stanford, Calif. 73.
RALL, W. 1967. *J. Neurophysiol.* **30**:1138.
RALL, W. 1969 *a. Biophys. J.* **9**:1483.
RALL, W. 1969 *b. Biophys. J.* **9**:1509.
RALL, W. 1970. *In* Excitatory Synaptic Mechanisms. P. Andersen, and J. K. S. Jansen, editors. Universitets Forlaget, Oslo. 175.
RALL, W., R. E. BURKE, T. G. SMITH, P. G. NELSON, and K. FRANK. 1967. *J. Neurophysiol.* **30**:1169.
RALL, W., and G. M. SHEPHERD. 1968. *J. Neurophysiol.* **31**:884.
RAMON-MOLINER, E. 1962. *J. Comp. Neurol.* **119**:211.
RAMON-MOLINER, E. 1968. *In* The Structure and Function of the Nervous System. G. H. Bourne, editor. Academic Press, Inc., New York. **1**:205.
SCHEIBEL, M. E., and A. B. SCHEIBEL. 1970. *Int. Rev. Neurobiol.* **13**:1.
SHOLL, D. A. 1953. *J. Anat.* **87**:387.
SHOLL, D. A. 1956. The Organization of the Cerebral Cortex. John Wiley and Sons, Inc., New York.
SPENCER, W. A., and E. R. KANDEL. 1961. *J. Neurophysiol.* **24**:260.
TAKAHASHI, K. 1965. *J. Neurophysiol.* **28**:908.
WUERKER, R. B., A. M. MCPHEDRAN, and E. HENNEMAN. 1965. *J. Neurophysiol.* **28**:85.